Akt phosphorylation of Deleted in Liver Cancer 1 abrogates its suppression of liver cancer tumorigenesis and metastasis

Frankie Chi Fat Ko, Lo-Kong Chan, Edmund Kwok-Kwan Tung, Scott W. Lowe, Irene Oi-Lin Ng, Judy Wai Ping Yam

PII: S0016-5085(10)00960-1
DOI: 10.1053/j.gastro.2010.06.051
Reference: YGAST 56407

To appear in: *Gastroenterology*

Received date: 5 January 2010
Revised date: 18 May 2010
Accepted date: 17 June 2010

Please cite this article as: Ko, F.C.F., Chan, L.K., Tung, E.K.K., Lowe, S.W., Ng, I.O.L., Yam, J.W.P., Akt phosphorylation of Deleted in Liver Cancer 1 abrogates its suppression of liver cancer tumorigenesis and metastasis, *Gastroenterology* (2009), doi: 10.1053/j.gastro.2010.06.051.

Akt phosphorylation of Deleted in Liver Cancer 1 abrogates its suppression of liver cancer tumorigenesis and metastasis

Short Title: Akt phosphorylates and deregulates DLC1

Frankie Chi Fat Ko[1,2], Lo-Kong Chan[1,2], Edmund Kwok-Kwan Tung[1,2], Scott W. Lowe[3,4], Irene Oi-Lin Ng[1,2,*], Judy Wai Ping Yam[1,2,*]

[1]Liver Cancer and Hepatitis Research Laboratory and SH Ho Foundation Research Laboratories, Department of Pathology, Li Ka Shing Faculty of Medicine, The University of Hong Kong, Hong Kong

[2]Centre for Cancer Research, Li Ka Shing Faculty of Medicine, The University of Hong Kong, Hong Kong

[3]Cold Spring Harbor Laboratory, Cold Spring Harbor, New York, 11724, USA

[4]Howard Hughes Medical Institute, Cold Spring Harbor, New York, 11724, USA

*Co-corresponding authors

Grant support

This work was supported by the Hong Kong Research Grants Council (HKU7798/07M), RGC Collaborative Research Grants (HKU 1/06C) and the University of Hong Kong Seed Funding Programme for Basic Research and Outstanding Young Researcher Award (to J.W.P. Yam). I.O.L. Ng is a Loke Yew Professor in Pathology.

Abbreviations used in this paper:

HCC, hepatocellular carcinoma; DLC1, deleted in liver cancer 1; RhoGAP, Rho GTPase activating protein; PKC, protein kinase C; PKD, protein kinase D; PI3K, phosphatidylinositol 3-kinase

Correspondence should be addressed to

Judy W.P. Yam

Department of Pathology, The University of Hong Kong, University Pathology Building, Queen Mary Hospital, Hong Kong.

Tel: (852) 2255-4864; Fax: (852) 2218-5212; E-mail: judyyam@pathology.hku.hk

Irene O.L. Ng

Room 127B, University Pathology Building, Department of Pathology, The University of Hong Kong, Queen Mary Hospital, Pokfulam, Hong Kong.

Tel: (852) 2255-4197; Fax: (852) 2872-5197; E-mail: iolng@hku.hk

Author contributions

F.C.F. Ko and J.W.P. Yam were involved in experimental design. F.C.F. Ko performed biochemical and animal experiments. L.K. Chan contributed to the immunofluorescence staining and rhotekin pull-down assays. S.W. Lowe provided the reagents and cell line for stable clone establishment. E.K.K. Tung assisted in the liver orthotopic implantation experiment. I.O.L. Ng performed the histological analysis of xenografts excised from animals. F.C.F. Ko and J.W.P. Yam wrote the manuscript. J.W.P. Yam and I.O.L. Ng provided project management. All authors discussed the results and commented on the manuscript.

Abstract

BACKGROUND & AIMS: Deleted in liver cancer 1 (DLC1), which encodes a Rho GTPase activating protein (RhoGAP), is a bona fide tumor suppressor in hepatocellular carcinoma (HCC). Underexpression of DLC1 in cancer has been attributed to genomic deletion and epigenetic silencing. However, the regulatory mechanism of the tumor suppressive activity of DLC1 remains elusive. In this study, we elucidated a novel post-translational modification by which the activity of DLC1 is functionally regulated. **METHODS:** Molecular and biochemical approaches were employed to study Akt phosphorylation of DLC1. *In vitro* and *in vivo* functional assays were performed to elucidate the functional significance of Akt phosphorylation of DLC1. **RESULTS:** Phosphorylation of ectopically expressed and endogenous DLC1 was enhanced upon insulin induction or with Akt expression in liver cancer cell lines. Conversely, addition of a PI3K/Akt pathway inhibitor or silencing of Akt attenuated the phosphorylation level of DLC1. Site-directed mutagenesis was employed to replace the serine residue of the consensus Akt substrate motifs of DLC1 with alanine. S567 of DLC1 was identified as the only target of Akt phosphorylation. S567 is well conserved in all DLC family members. DLC2 was phosphorylated by Akt at the corresponding residue. Functional assays demonstrated that the S567D phosphomimetic DLC1 mutant lost its inhibitory activities in tumorigenesis and metastasis of oncogenically transformed hepatoblasts in a mouse model. **CONCLUSIONS:** This study has revealed a novel post-translational modification that functionally deregulates the biological activities of DLC1. Phosphorylation of DLC1 and DLC2 by Akt at the conserved residue points to a common regulatory mechanism of the DLC tumor suppressor family.

Keywords: Deleted in liver cancer 1; Akt; phosphorylation; hepatocellular carcinoma

Introduction

Deleted in liver cancer 1 (DLC1) was identified as a putative tumor suppressor in hepatocellular carcinoma (HCC) in 1998[1]. Since its identification, accumulating evidence has shown that DLC1 is not only involved in HCC, but also in diverse human cancers[2]. DLC1 is a focal adhesion protein and functions as a Rho GTPase activating protein (RhoGAP)[3]. Localization at focal adhesions, interaction with tensin proteins and RhoGAP activity are crucial to the tumor suppressor functions of DLC1[4-8]. When ectopically expressed in cancer cells, DLC1 inhibits proliferation and induces apoptosis[7, 9-12]. Furthermore, DLC1 abrogates cell motility and functions as a suppressor of metastasis in cancer cells[7, 13-15]. Conversely, depletion of DLC1 in cells enhances growth and motility potential[16, 17]. Functional data about the loss of DLC1 in HCC tumorigenesis using a knockdown approach was recently demonstrated in a mouse model[18].

DLC1 is widely expressed in normal human tissues, but it is frequently underexpressed in HCC and other cancers. Heterozygous deletion and promoter hypermethylation of DLC1 are commonly found in about 30-50% of prostate[19], breast[20] and liver cancers[21, 22]. Other mechanisms could possibly be involved in the regulation of DLC1 activity in tumor tissues with normal expression of DLC1. Indeed, somatic mutations of DLC1 have been recently detected in human prostate cancers[23]. These mutations localize in the focal adhesion targeting region and impair the RhoGAP activity of DLC1. Although DLC1 expression has been well documented to be regulated at the transcriptional level, a recent study about regulation of the activity and compartmentalization of DLC1 by protein kinases has provided evidence that DLC1 activity could be regulated by post-translational modification. Activated protein kinase C (PKC) and protein kinase D (PKD) stimulate the association between DLC1 and 14-3-3

proteins. Enhanced association blocks DLC1 nucleocytoplasmic shuttling and inhibits the RhoGAP activity of DLC1[24]. Moreover, identification of the rat homolog of DLC1, p122RhoGAP, as a substrate of Akt has provided insights into a potential regulatory pathway of DLC1[25]. However, the functional significance Akt phosphorylation of p122RhoGAP and its relevance to human DLC1 have not been investigated. The phosphatidylinositol 3-kinase (PI3K)/Akt pathway is an important cell survival cascade. An aberrant Akt signaling pathway and downstream effectors have been shown to have crucial roles in human cancers[26]. Here, we hypothesized that Akt is involved in the regulation of the tumor suppression activity of DLC1 in HCC. In this study, we elucidated the molecular mechanism of Akt phosphorylation of DLC1 in liver cancer cells and determined the functional significance of hyperphosphorylated DLC1 in oncogenically transduced mouse hepatoblasts.

Materials and Methods

Constructs and reagents

Expression constructs of Myc-tagged wild-type DLC1 (1-1091), deletion mutants (1-292, 1-595, 1-807, 292-1091, 648-1091, Δ414-432), the RhoGAP mutant (K714E) and GFP-tagged DLC2α were constructed as previously described[7, 8, 27]. DLC1 internal deletion mutants (Δ292-353, Δ292-646, Δ375-509 and Δ414-432), phospho-defective mutants (S298A, S329A, S432A and S567A) and the phosphomimetic mutant (S567D) as well as wild-type DLC2α and the DLC2α phospho-defective mutant (S589A) were generated. Wild-type DLC1, S567A and S567D fragments were subcloned into the MSCV-PGK-PIG vector harboring a 6×Myc tag at the N-terminus[18]. The full-length Akt1 fragment was amplified from normal human liver cDNA. A PCR-based site-directed mutagenesis method was used to generate the constitutively active mutant (E17K)[28], the kinase dead mutant (K179M) and the phospho-defective mutant (AA, T308AS473A). Amplified fragments were cloned into pCS+MT and FLAG-pcDNA3.1(+) (Invitrogen, Carlsbad, CA) expression vectors. Primers employed in cloning are listed in Supplementary Information, Table 1. Monoclonal anti-β-actin, anti-FLAG and anti-vinculin antibodies were from Sigma-Aldrich (St. Louis, MO). Recombinant Akt protein, the Akt *in vitro* kinase assay kit and antibodies against total Akt, phospho-Akt (Ser-473) and phospho-Akt substrate (PAS) were from Cell Signaling Technology (Danvers, MA). Anti-Myc and anti-DLC1 antibodies were from Santa Cruz Biotechnology (Santo Cruz, CA) and BD Biosciences (San Jose, CA), respectively. LY294002 was from Calbiochem (San Diego, CA) and insulin was from Novo Nordisk (Denmark).

Cell culture

The human embryonic kidney cell line, HEK293T, and hepatocellular adenoma cells, SK-Hep-1, were purchased from American Type Culture Collection (Manassas, VA), whereas the human HCC cell line, SMMC-7721, was obtained from the Shanghai Institute of Cell Biology. HEK293T, SMMC-7721 and SK-Hep-1 cells were cultured in DMEM high glucose medium supplemented with 10% (v/v) fetal bovine serum, penicillin, and streptomycin at 37°C in a humidified incubator with 5% CO_2 in air. Mouse $p53^{-/-}$;RasV12 hepatoblasts were cultured as previously described[18]. MSCV-PGK-PIG retroviral constructs of wild-type and mutant DLC1 were transfected into PA317 cells for retroviral packaging. Transfection with the indicated plasmid was done with Lipofectamine 2000 (Invitrogen, Carlsbad, CA). Viral particles were collected from the medium. Mouse $p53^{-/-}$;RasV12 hepatoblasts were transduced by retroviral particles in the presence of polybrene. Stable cell lines were established under 1 μg/ml puromycin selection for 1-2 weeks. Phosphorylation of DLC1 was induced by 50-100 nM of insulin for 30 minutes before collecting cells for protein extraction. Inhibition of phosphorylation was carried out by pre-treating cells with 10 μM of LY294002 or other inhibitors as controls for 1 h before insulin stimulation.

Colony formation assay

SMMC-7721 cells were seeded at 1×10^5 per well into 12-well tissue culture plates. One of the DLC1 expression vectors (pCS2+MT, DLC1-pCS2+MT, DLC1S567A-pCS2+MT or DLC1S567D-pCS2+MT) was co-transfected with 0.2 μg of pcDNA3.1+(neo) into cells. Cells were trypsinized and replated in a 1:20 dilution in triplicates one day after transfection. Cells were selected in 700 μg/ml of G418 (Merck, Darmstadt, Germany) for three weeks. Colonies formed were fixed with 3.7% formaldehyde and stained with crystal violet solution.

Subcutaneous injection and orthotopic liver implantation in nude mice

In vivo tumorigenicity of mouse hepatoma $p53^{-/-}$;RasV12 cells stably transfected with DLC1, S567A or S567D was analyzed by injection into nude mice. For these experiments, $1x10^5$ cells were inoculated into the right flank of 5-week-old female BALB/c nude mice. Four injections were performed for each group. Tumor size was monitored twice a week for 14 days. Tumor volume was estimated according to the following formula: volume = 1/2 (largest diameter) × $(\text{smallest diameter})^2$. Tumors formed were resected two weeks after subcutaneous injection for orthotopic liver implantation. The tumors were cut into 1-2 mm^3 cubes then implanted in liver lobes of the nude mice as previously described[29]. Four implantations were performed per cell line. All animals were sacrificed and examined three weeks after implantation. The *in vivo* tumor formation was detected by bioluminescence. D-luciferin (Xenogen, Hopkinton, MA) at 100 mg per kg of animal was injected intraperitoneally into the mice, and bioluminescence was detected by an IVIS 100 Imaging System (Xenogen). The experiment was performed according to the Animals (Control of Experiments) Ordinance (Hong Kong) and followed the University's guidelines on animal experimentation. The diameter of each tumor formed in livers was taken as a measure of tumor size. Livers and lungs were excised and fixed in 10% formalin followed by 75% ethanol before paraffin embedding. Five-micrometer-thick paraffin sections were cut and stained with hematoxylin-eosin for histological examination. Tumors formed were analyzed histologically for the presence of any aggressive features such as an invasive tumor front and venous invasion. Lungs of mice were analyzed macroscopically or microscopically for any established metastasis.

Protein extraction, co-immunoprecipitation and western blotting

Experimental details of protein lysis, co-immunoprecipitation and western blotting have been previously described[27]. Ectopically expressed epitope-tagged proteins were

immunoprecipitated from total cell lysates using antibodies against the tagged epitope, and the endogenous DLC1 protein was immunoprecipitated by an anti-DLC1 antibody. Immunoprecipitated proteins were subjected to western blotting, and phosphorylation signals were determined using the PAS antibody (Cell Signaling).

In vitro kinase assay

The *in vitro* kinase assay was performed using an Akt kinase assay kit (Cell Signaling Technology) according to the manufacturer's manual with slight modifications. Recombinant GST-DLC1 protein was generated by a GST expression system. GST-DLC1 or immunoprecipitated Myc-tagged DLC1 was washed twice in 1× kinase buffer (25 mM Tris, pH 7.5, 5 mM β-glycerophosphate, 2 mM DTT, 0.1 mM Na_3VO_4, 10 mM $MgCl_2$). In the 50-ml reaction, 0.2-0.5 mg of DLC1 protein was incubated with 0.2 mM ATP with or without 0.2 mg of GST-Akt1 at 30°C for 30 minutes. The reaction was stopped by adding 10 ml 6× protein loading dye and boiling for five minutes. The phosphorylation signal was detected using the PAS antibody for western blotting. A known Akt substrate, recombinant GSK, was used as a positive control.

Statistical analysis

Student's *t*-test analysis by GraphPad Prism 5.02 (San Diego, California, USA) was used to determine the difference between the results of experimental groups with those of the control. A *P*-value less than 0.05 was regarded as statistically significant. Mean and standard deviation (s.d.) of each group were calculated and shown.

Results

DLC1 is a substrate of Akt

ScanProsite protein sequence analysis of DLC1 revealed the presence of three characteristic phospho-Akt substrate (PAS) motifs, (R/K)XRXX(S*/T*) (R: arginine; K: lysine; S* and T*: phosphorylated serine and threonine; and X: any amino acid) at amino acids 293-298 (RKRSVS*), 324-329 (RTRSLS*) and 562-567 (RLRWHS*) of DLC1 (Figure 1*A*). Three potential Akt phosphorylation serine residues, S298, S329 and S567, are all localized in the central region of DLC1 and are conserved among human DLC1 and rat p122RhoGAP. S329 corresponds to S322 of the rat homolog, which was previously reported to be phosphorylated by Akt[25]. To elucidate whether Akt also phosphorylates human DLC1, we employed an antibody against PAS to detect the phosphorylation of DLC1. The phosphorylation was detected in ectopically expressed Myc-DLC1 in HEK293T cells. The phosphorylation was enhanced by insulin stimulation (Figure 1*B*) or Akt co-transfection (Figure 1*C*) while dramatically reduced when the cell lysate was treated with alkaline phosphatase (Supplementary Figure 1). The phosphorylation of endogenous DLC1 was verified in the SK-Hep-1 hepatoadenocarcinoma cell line, in which DLC1 expression is high. The phosphorylation was detected in immunoprecipitated endogenous DLC1 (Figure 1*D*). Insulin stimulation enhanced DLC1 phosphorylation, whereas addition of the PI3K inhibitor LY294002 reduced the phosphorylation. Depletion of Akt also suppressed phosphorylation of DLC1 (Figure 1*E*). An *in vitro* kinase assay further demonstrated phosphorylation of DLC1 by recombinant Akt1 (Figure 1*F*; Supplementary Figure 2). Basal phosphorylation signal was detected in immunoprecipitated DLC1. Presumably, this is due to endogenous Akt activity in the cells.

Akt phosphorylates DLC1 at S567

To identify the Akt-phosphorylated residue(s) in DLC1, a panel of DLC1 deletion mutants was examined for the phosphorylation signal (Figure 2*A*). Loss of the PAS signal in the Δ292-646 mutant suggested that the phosphorylated residue(s) was located in amino acids 292-646 of DLC1 (Figure 2*B*). Detection of the signal in the Δ292-353 mutant, in which S298 and S329 were removed, implicated that S567 was the potential Akt-phosphorylated residue. In addition, detection of signal in the 400-1091, 450-1091 and 500-1091 mutants but not in the 648-1091 mutant further supported that S567 was the phosphorylation target (Supplementary Figure 3). Intriguingly, the PAS signal could not be detected in C-terminal deletion mutants, such as 1-595, 1-807, 1-878, 1-989, suggesting that an intact START domain is required for phosphorylation of DLC1 by Akt (Figure 2*C*; Supplementary Figure 3*B*). However, the functional significance of the START domain in Akt phosphorylation of DLC1 remains to be further investigated. Direct phosphorylation of DLC1 by Akt was confirmed by the *in vitro* kinase assay using recombinant Akt1 and GST-DLC1 500-1091 and 500-878 fusion proteins (Figure 2*D*).

In order to validate that S567 is the target of Akt phosphorylation, phospho-defective mutants (S298A, S329A, S567A) with an alanine substitution of S298, S329 and S567, respectively, were created (Figure 2*A*). The phosphorylation was completely absent in the S567A mutant, whereas a strong signal was detected in wild-type DLC1 as well as in both S298A and S329A mutants (Figure 2*E*). In addition, co-transfection with Akt dramatically enhanced the phosphorylation in all DLC1 constructs, with the exception of S567A. Consistently, recombinant Akt1 strongly phosphorylated immunoprecipitated Myc-tagged DLC1, S298A and S329A, but not S567A (Figure 2*F*).

Akt phosphorylates DLC2 at the corresponding residue to DLC1 S567

DLC family members (DLC1, DLC2 and DLC3) are structurally conserved with high sequence homology[30] (Figure 3*A*). Sequence analysis also revealed the presence of putative PAS motifs in amino acids 253-258 (RARAKS*), 567-572 (RDRRDS*) and 584-589 (RLRWHS*) of DLC2 and in amino acids 203-208 (RHRNRS*), 556-561 (RERRDS*) and 563-578 (KLRWHS*) of DLC3. Among all putative PAS motifs, S567 of DLC1 is the only putative phosphorylation residue to be conserved in the family. S567 of DLC1 corresponds to S589 of DLC2 and S578 of DLC3 (Figure 3*A*). We found that the phosphorylation was also detected in DLC2 and was enhanced when DLC2 was co-transfected with Akt (Figure 3*B*). Substitution of S589 with alanine completely abolished the phosphorylation and suggests that Akt phosphorylates DLC2 at the corresponding S589.

DLC1 interacts with Akt

Demonstration of Akt phosphorylation of DLC1 prompted us to further investigate whether DLC1 interacts with Akt. Co-immunoprecipitation confirmed interaction between ectopically expressed DLC1 and Akt (Figure 4*A*). Apart from wild-type Akt, only the constitutively active Akt E17K mutant could robustly interact with DLC1, but the kinase dead Akt, K179M, and phospho-defective, T308AS473A (AA), mutant failed to associate with DLC1. This result revealed the requirement of Akt kinase activity in DLC1-Akt association. In accordance with this finding, DLC1 was only phosphorylated by wild-type and constitutively active Akt. Endogenous Akt was shown to interact with Myc-DLC1, and the interaction of these proteins was enhanced upon insulin stimulation (Figure 4*B*). We also questioned whether the phosphorylation status of DLC1 would affect its interaction with Akt. Our result showed that S567A had largely reduced interaction whereas S567D displayed a stronger binding with Akt compared to the wild-type DLC1 (Figure 4*C*). This suggests that

S567 phosphorylation status of DLC1 correlates to its binding with Akt. Another serine residue, S432, resides in a pseudo-site with a sequence (KRRNSS*) similar to the consensus PAS motif. Substitution of S432 with alanine also did not affect the DLC1-Akt interaction, and this further supports the idea that the DLC1-Akt interaction is specifically determined by phosphorylation at S567 (Figure 4*D*).

Akt phosphorylation of DLC1 regulates its growth suppression activity

DLC1 has been well documented to inhibit cell growth when ectopically expressed in various cancer cell lines[7, 23, 31, 32]. To determine the functional significance of phosphorylation of DLC1 at S567, we performed a colony formation assay using SMMC-7721 cells to compare the growth suppression activities of DLC1 with its mutants (Figure 5*A*). The S567A mutant inhibited colony formation as efficiently as wild-type DLC1. Both the RhoGAP mutant K714E and the phosphomimetic mutant S567D lost the ability to inhibit colony formation. The growth suppression activity of DLC1 was also assessed by colony formation assays and proliferation curves in an activated Akt background. These assays revealed that wild-type DLC1 lost growth inhibitory activity, whereas the S567A mutant retained its ability to suppress HCC cell growth (Supplementary Figure 4). Our findings implicate that phosphorylation at S567 by Akt deregulates the activity of DLC1 in suppressing cell growth.

Recently, functional data about the loss of DLC1 in HCC tumorigenesis using specific short-hairpin RNA interference were first demonstrated in a mouse model[18]. To determine the physiological relevance of DLC1 phosphorylation in tumorigenicity, we stably expressed DLC1 and its mutants in a mouse p53-null hepatoblast cell line expressing an oncogenic Ras ($p53^{-/-}$;RasV12) labeled with luciferase (Figure 5*B*). Compared with the control cells, DLC1 and S567A dramatically suppressed cell growth (Figure 5*C*) and anchorage-independent

growth (Figure 5*D*). In contrast, S567D displayed largely attenuated growth suppression activity when compared to DLC1 and S567A. S567D cells grew faster and formed more and bigger colonies. DLC1 has been shown to induce apoptosis in an HCC cell line[12]. To investigate whether Akt phosphorylation affects the apoptosis-inducing activity of DLC1, stable clones of DLC1 were subjected to flow cytometry and TUNEL staining (Supplementary Figure 5). The data showed a higher percentage of subG1 population and more positive TUNEL-stained cells were detected in DLC1 and S567A cells when compared with the control and S567D cells. Moreover, wildtype DLC1 was shown to lose its ability to induce apoptosis in hepatoma cells with activated Akt background. The stable clones of DLC1 and its mutants were then injected subcutaneously into nude mice and tested for their *in vivo* tumorigenicity (Figure 5*E*). Both wild-type DLC1 and the S567A mutant efficiently suppressed tumor formation, whereas S567D mutant formed the biggest tumors among all experimental groups (Figure 5*F*).

Solid tumors excised from subcutaneous injection were subjected to orthotopic liver implantation. Three weeks after implantation, luciferase imaging revealed inhibition of tumor growth by wild-type DLC1 and the S567A mutant when compared to the control. In contrast, the S567D mutant accelerated tumor growth (Figure 6*A*). In accordance with the luciferase signal, wild-type DLC1 and the S567A mutant formed smaller tumors whereas S567D formed the largest tumors among all groups (Figure 6*B*). Wild-type DLC1 and the S567A mutant delayed tumor onset *in vivo*. Because of the enormous tumor formation, animals of S567D group were the first to die (Figure 6*C*). Examination of the livers revealed that tumor microsatellite formation was found in two out of four mice from the S567D group in contrast to only a single focus of microsatellite formation found in just one mouse each in the vector and wild-type groups (Figure 6*D* and 6*F*). Distant metastases in the lungs were found in all

mice from the S567D group and in none of the mice in the wild-type group (Figure 6*E* and 6*F*). In the S567D group, large foci of lung metastasis were found in three mice, and a total of 10 large foci were observed. Although lung metastases were found in two mice in each of the vector and S567A groups, large foci were found in two mice, and a total of 12 foci were formed in the vector group. However, in two mice of the S567A group, mostly micrometastases were observed, and only two large foci were found in the whole group. Collectively, the incidence of lung metastases and aggressive features were reduced in tumors derived from the wild-type and S567A groups. Our data revealed that both wild-type and S567A mutant DLC1 efficiently suppressed the metastatic potentials of hepatoma cells but that the S567D mutant lost the inhibitory ability to suppress metastasis.

Discussion

In this study, we have shown that Akt is a novel regulator of DLC1. Activated Akt interacted with and phosphorylated DLC1 at S567. Hyper-phosphorylated DLC1 lost its tumor suppressive activity in tumorigenesis and metastasis (Figure 7). A previous study reported that Akt phosphorylates rat DLC1, p122RhoGAP, at S322[25]. However, our data showed that Akt did not phosphorylate S329 (which corresponds to S322 of p122RhoGAP), but that instead, S567 is the major target of Akt. This reflects differential regulatory signaling pathways in rat and human DLC1 or in different cell types. In spite of the differential regulation between orthologs, our data showed that Akt also phosphorylated the corresponding residue in another human DLC family member, DLC2. Although we did not provide evidence about Akt phosphorylation of DLC3, conservation of S567 of DLC1 with the corresponding residues in DLC2 and DLC3 implies that DLC3 could also be

phosphorylated by Akt. Our findings here have provided the first evidence about the importance of S567 and point to a common regulatory mechanism in the DLC family.

All DLC family members share a similar structural organization, including the presence of a sterile alpha motif (SAM) domain at the amino-terminus as well as RhoGAP and steroidogenic acute regulatory (StAR)-related lipid transfer (START) domains at the carboxyl-terminus. The central region between the SAM and RhoGAP domains is less conserved among family members and has no specialized structural domain[30]. Nevertheless, the central region has been shown to be responsible for focal adhesion localization and interaction with tensins, events which are crucial to the growth suppression activity[5, 6, 8, 27]. The central region of DLC1 has been shown to be phosphorylated by PKC/PKD[24]. Phosphorylation of DLC1 by PKC and PKD enhances its interaction with the 14-3-3 adaptor protein. Association with 14-3-3 inhibits the RhoGAP activity and facilitates the cytosolic retention of DLC1. Our findings have further implicated the importance of the central region of DLC1 for post-translational modification that is crucial for its tumor suppressive capacities. The present study has shown that phosphorylation of DLC1 at S567 by Akt reduced the ability of DLC1 to inhibit the cell growth of both human HCC cells *in vitro* and mouse hepatoblasts *in vivo* as well as the metastasis of the latter. The inhibitory function of DLC1 in cancer cell metastasis has been reported in breast cancer cells[13]. In this study, we demonstrated that DLC1 also functions as a negative regulator of mouse hepatoma metastasis.

In the physiological context, enhanced activation of Akt through phosphorylation at S473 in clinical HCC samples has been detected and correlated with poorer overall survival[33]. Apart from down-regulation of DLC1 expression observed in about 50% of cancers[21, 22], enhanced phosphorylation levels of DLC1 could be an indicator for functionally deregulated DLC1 in

cases with normal expression level of DLC1. Elevated expression levels and hyperactivation of Akt have been observed in many human cancers[34], and DLC1 has been shown to be functionally involved in diverse human cancers. In this regard, deregulation of DLC1 tumor suppressor functions by enhanced activation of Akt is implicated in a broad spectrum of human cancers. In order to validate the altered Akt/DLC1 signaling pathway in human cancerous tissues, generation of specific phospho-DLC1 (S567) antibody will be an indispensable tool. Due to the failure in generating the phospho-DLC1 after several attempts, the study of the enhanced phosphorylation of DLC1 in human cancers cannot be accomplished at present and awaits investigation in future.

Focal adhesion localization and RhoGAP activity have been demonstrated to have crucial roles in the tumor suppression activity of DLC1[5, 6, 8, 11, 23, 35]. However, our data revealed that the focal adhesion localization and RhoGAP activity of DLC1 were not affected by phosphorylation by Akt. Immunofluorescence staining revealed that, similar to wild-type DLC1, both S567A and S567D mutants displayed punctate patterns at the boundary that perfectly co-localized with vinculin in SMMC-7721 cells (Supplementary Figure 6*A*). RhoGAP activity of DLC1 could be reflected by its ability to inhibit RhoA activity and stress fiber formation[7, 23, 35, 36]. Upon transient transfection, wild-type DLC1 inhibited serum-induced stress fiber formation in SMMC-7721 cells, but the K714E RhoGAP mutant lost the ability to suppress stress fiber formation (Supplementary Figure 6*B*). Both S567A and S567D inhibited stress fiber formation as efficiently as wild-type DLC1. Consistently, a rhotekin pull-down assay showed that RhoA activity was inhibited in all stable HCC clones of wild-type and mutant DLC1 (Supplementary Figure 6*C*). Collectively, in spite of the deregulation of DLC1 tumor suppression functions by Akt phosphorylation, the RhoGAP activity of DLC1 was not affected. Indeed, mediation of growth suppression activity via

RhoGAP-independent mechanisms has been implicated in non-small cell lung cancer (NSCLC) cells[15]. Expression of a GAP-deficient DLC1 mutant also inhibited anchorage-independent growth and invasion of NSCLC cells, although to a lesser extent than the wild-type DLC1 did. Abrogation of the tumor suppressive activity of DLC1 by Akt phosphorylation through a RhoGAP-independent pathway suggests that DLC1 is potentially involved in other, undefined mechanisms, which await further investigation.

Figure Legends

Figure 1. Akt phosphorylates DLC1. (*A*) Schematic representation of three putative phospho-Akt substrate motifs and potential Akt phosphorylation residues, S298, S329 and S567, in the central region of DLC1. (*B*) Detection of phosphorylation signal of DLC1. Under insulin stimulation, Myc-DLC1 expressed in HEK293T cells was immunoprecipitated (IP) by Myc antibody and detected by phospho-Akt substrate (PAS) antibody. The signal detected was enhanced upon insulin stimulation. (*C*) Positive signal detected by PAS antibody was also enhanced when DLC1 was co-expressed with Akt. (*D*) Endogenous DLC1 in SK-Hep-1 cells was immunoprecipitated by DLC1 antibody and subjected to western blotting using PAS antibody. Phosphorylation was elevated upon insulin stimulation and was reduced by LY294002 treatment. (*E*) Depletion of Akt by siRNA suppressed phosphorylation of DLC1. (*F*) Immunoprecipitated Myc-DLC1 was phosphorylated by recombinant Akt1 in an *in vitro* kinase assay.

Figure 2. Akt phosphorylates DLC1 at S567. (*A*) Schematic diagram of DLC1 and its mutants. (*B*) Different Myc-DLC1 constructs expressed in HEK293T cells were immunoprecipitated

by Myc antibody and detected by PAS antibody. Loss of PAS signal in the Δ292-646 mutant and positive signal detected in the Δ292-353 mutant implicated that S567 may be the main phosphorylation target. (*C*) C-terminal deletion mutants of DLC1 with intact PAS motif(s) could not be phosphorylated by Akt. (*D*) *In vitro* kinase assay showing purified GST-DLC1 fusion proteins (500-1091, 500-878) incubated with or without recombinant Akt1 in the presence of ATP. The phosphorylation was detected using PAS antibody by western blotting. Akt could directly phosphorylate DLC1. (*E*) HEK293T cells co-transfected with DLC1 or phospho-defective mutants (S298A, S329A and S567A) and FLAG-Akt were subjected to immunoprecipitation by Myc antibody and immunoblotted with PAS antibody. PAS signal was completely lost in the S567A mutant. (*F*) Recombinant Akt1 could only phosphorylate immunoprecipitated S298A and S329A, but not S567A.

Figure 3. Akt phosphorylates another DLC family member, DLC2 (*A*) Putative PAS motifs in DLC family members. Potential phosphorylation residues are marked by asterisks. Only S567 of DLC1, corresponding to S589 of DLC2 and S578 of DLC3, was conserved among the family. (*B*) Wild-type DLC2 (WT) and its phospho-defective mutant (S589A) were expressed in HEK293T cells with or without FLAG-Akt. Cell lysates were immunoprecipitated with Myc antibody and immunoblotting with PAS antibody. PAS signal detected in the immunoprecipitated Myc-DLC2 was enhanced in the presence of Akt. The PAS signal was completely lost in the S589A mutant.

Figure 4. Association between DLC1 and Akt. (*A*) Akt activity is essential for the interaction between DLC1 and Akt. HEK293T cells were co-transfected with different forms of FLAG-Akt (WT: wild-type; E17K: constitutively active; K179M: kinase-dead; AA: phospho-defective) and Myc-DLC1. Cell lysates was subjected to immunoprecipitation.

DLC1 could only interact with the wild-type and constitutive active Akt, but not the kinase-dead and phospho-defective Akt. PAS could only be detected in DLC1 that associated with Akt. (*B*) Insulin stimulation enhanced the interaction between DLC1 and Akt. (*C*) Myc-DLC1 constructs (WT, S567A and S567D) were transfected with FLAG-Akt into HEK293 cells and cells were subjected to immunoprecipitation. The S567A mutant showed a weaker interaction with Akt than wild-type DLC1. The S567D mutant had the strongest interaction with Akt. (*D*) Another serine residue, S432, resides in a pseudo-site with the sequence KRRNSS*, which is similar to the consensus Akt substrate motif. The Myc-DLC1 mutant S432A was expressed in HEK293 cells with FLAG-Akt and examined for its interaction with Akt.

Figure 5. Akt phosphorylation attenuated growth suppression activities of DLC1. (*A*) Different DLC1 constructs were expressed in SMMC-7721 cells and grown in selective medium for two weeks. Numbers of colonies formed were counted. (*B*) Stable expression of DLC1 in $p53^{-/-}$;RasV12 hepatoma cells was confirmed by western blot analysis using Myc antibody. (*C*) Growth curves of $p53^{-/-}$;RasV12 hepatoma cells expressing different forms of DLC1. S567D had a faster proliferation rate than DLC1 and S567A. (*D*) DLC1 and S567A formed significantly fewer colonies than the vector control in a soft agar assay. (*E*) DLC1 stable clones were inoculated into nude mice, and tumor size was measured three times a week. (*F*) Tumors were excised and weighed at the end of experiments. H&E staining of representative tumors is shown. Mean ± s.d. of values were calculated and shown. Data were analyzed by Student's *t*-test, and $P<0.05$ was considered as statistically significant.

Figure 6. Metastasis inhibitory activity of DLC1 was abrogated by phosphorylation by Akt. (*A*) Orthotopic liver implantation of hepatoma cells stably expressing DLC1.

Bioluminescence images were detected by IVIS 100 Imaging System (Xenogen). (*B*) Livers were resected and the size of the tumor formed was measured and plotted. Mean ± s.d. of values were calculated and shown. Data were analyzed by Student's *t*-test, and $P<0.05$ was considered as statistically significant. (*C*) Survival of mice with orthotopic liver implantation of tumors derived from hepatoma cells stably expressing DLC1 (n = 8 for each group). Asterisks indicate that DLC1 and S567A were significantly different from vector control. (*D*) Tumors formed in liver of the wild-type DLC1 group displayed bulging growth fronts. Microsatellite formation (indicated by arrows) detected in S567D tumors. (*E*) Lungs were excised and examined for tumor nodules formation. (*F*) Summary of aggressive features of the orthotopic liver-implanted tumors.

Figure 7. Activated Akt pathway induces phosphorylation of DLC family members. Activated Akt phosphorylates DLC1 at S567. This putative phosphorylated serine residue is well conserved in the DLC family. S567 of DLC1 corresponds to S589 of DLC2 and S578 of DLC3. DLC2 was shown to be phosphorylated at S589 as well. Hyper-phosphorylated DLC1 lost its tumor suppression activities in tumorigenesis and metastasis of mouse $p53^{-/-}$;RasV12 hepatoma cells.

References

1. Yuan BZ, Miller MJ, Keck CL, et al. Cloning, characterization, and chromosomal localization of a gene frequently deleted in human liver cancer (DLC-1) homologous to rat RhoGAP. Cancer Res 1998;58:2196-2199.
2. Durkin ME, Yuan BZ, Zhou X, et al. DLC-1:a Rho GTPase-activating protein and tumour suppressor. J Cell Mol Med 2007;11:1185-1207.
3. Lahoz A, Hall A. DLC1: a significant GAP in the cancer genome. Genes Dev 2008;22:1724-1730.
4. Chan LK, Ko FCF, Ng IOL, et al. Deleted in liver cancer 1 (DLC1) utilizes a previously undocumented binding site for tensin2 PTB domain interaction and required for tumor suppressive function. PLoS ONE 2009.
5. Liao YC, Si L, deVere White RW, et al. The phosphotyrosine-independent interaction of DLC-1 and the SH2 domain of cten regulates focal adhesion localization and growth suppression activity of DLC-1. J Cell Biol 2007;176:43-49.
6. Qian X, Li G, Asmussen HK, et al. Oncogenic inhibition by a deleted in liver cancer gene requires cooperation between tensin binding and Rho-specific GTPase-activating protein activities. Proc Natl Acad Sci U S A 2007;104:9012-9017.
7. Wong CM, Yam JW, Ching YP, et al. Rho GTPase-activating protein deleted in liver cancer suppresses cell proliferation and invasion in hepatocellular carcinoma. Cancer Res 2005;65:8861-8868.
8. Yam JW, Ko FC, Chan CY, et al. Interaction of deleted in liver cancer 1 with tensin2 in caveolae and implications in tumor suppression. Cancer Res 2006;66:8367-8372.
9. Ng IO, Liang ZD, Cao L, et al. DLC-1 is deleted in primary hepatocellular carcinoma and exerts inhibitory effects on the proliferation of hepatoma cell lines with deleted

DLC-1. Cancer Res 2000;60:6581-6584.

10. Yuan BZ, Durkin ME, Popescu NC. Promoter hypermethylation of DLC-1, a candidate tumor suppressor gene, in several common human cancers. Cancer Genet Cytogenet 2003;140:113-117.

11. Yuan BZ, Jefferson AM, Baldwin KT, et al. DLC-1 operates as a tumor suppressor gene in human non-small cell lung carcinomas. Oncogene 2004;23:1405-1411.

12. Zhou X, Thorgeirsson SS, Popescu NC. Restoration of DLC-1 gene expression induces apoptosis and inhibits both cell growth and tumorigenicity in human hepatocellular carcinoma cells. Oncogene 2004;23:1308-1313.

13. Goodison S, Yuan J, Sloan D, et al. The RhoGAP protein DLC-1 functions as a metastasis suppressor in breast cancer cells. Cancer Res 2005;65:6042-6053.

14. Kim TY, Healy KD, Der CJ, et al. Effects of structure of Rho GTPase-activating protein DLC-1 on cell morphology and migration. J Biol Chem 2008.

15. Healy KD, Hodgson L, Kim TY, et al. DLC-1 suppresses non-small cell lung cancer growth and invasion by RhoGAP-dependent and independent mechanisms. Mol Carcinog 2008;47:326-337.

16. Heering J, Erlmann P, Olayioye MA. Simultaneous loss of the DLC1 and PTEN tumor suppressors enhances breast cancer cell migration. Exp Cell Res 2009;315:2505-2514.

17. Holeiter G, Heering J, Erlmann P, et al. Deleted in liver cancer 1 controls cell migration through a Dia1-dependent signaling pathway. Cancer Res 2008;68:8743-8751.

18. Xue W, Krasnitz A, Lucito R, et al. DLC1 is a chromosome 8p tumor suppressor whose loss promotes hepatocellular carcinoma. Genes Dev 2008;22:1439-1444.

19. Guan M, Zhou X, Soulitzis N, et al. Aberrant methylation and deacetylation of deleted in liver cancer-1 gene in prostate cancer: potential clinical applications. Clin Cancer

Res 2006;12:1412-1419.

20. Plaumann M, Seitz S, Frege R, et al. Analysis of DLC-1 expression in human breast cancer. J Cancer Res Clin Oncol 2003;129:349-354.

21. Ko FC, Yeung YS, Wong CM, et al. Deleted in liver cancer 1 isoforms are distinctly expressed in human tissues, functionally different and under differential transcriptional regulation in hepatocellular carcinoma. Liver Int 2009.

22. Wong CM, Lee JM, Ching YP, et al. Genetic and epigenetic alterations of DLC-1 gene in hepatocellular carcinoma. Cancer Res 2003;63:7646-7651.

23. Liao YC, Shih YP, Lo SH. Mutations in the focal adhesion targeting region of deleted in liver cancer-1 attenuate their expression and function. Cancer Res 2008;68:7718-7722.

24. Scholz RP, Regner J, Theil A, et al. DLC1 interacts with 14-3-3 proteins to inhibit RhoGAP activity and block nucleocytoplasmic shuttling. J Cell Sci 2009;122:92-102.

25. Hers I, Wherlock M, Homma Y, et al. Identification of p122RhoGAP (deleted in liver cancer-1) Serine 322 as a substrate for protein kinase B and ribosomal S6 kinase in insulin-stimulated cells. J Biol Chem 2006;281:4762-4770.

26. Manning BD, Cantley LC. AKT/PKB signaling: navigating downstream. Cell 2007;129:1261-1274.

27. Chan LK, Ko FC, Ng IO, et al. Deleted in liver cancer 1 (DLC1) utilizes a novel binding site for Tensin2 PTB domain interaction and is required for tumor-suppressive function. PLoS One 2009;4:e5572.

28. Carpten JD, Faber AL, Horn C, et al. A transforming mutation in the pleckstrin homology domain of AKT1 in cancer. Nature 2007;448:439-444.

29. Yam JW, Ko FC, Chan CY, et al. Tensin2 variant 3 is associated with aggressive tumor behavior in human hepatocellular carcinoma. Hepatology 2006;44:881-890.

30. Durkin ME, Ullmannova V, Guan M, et al. Deleted in liver cancer 3 (DLC-3), a novel Rho GTPase-activating protein, is downregulated in cancer and inhibits tumor cell growth. Oncogene 2007;26:4580-4589.

31. Kim TY, Lee JW, Kim HP, et al. DLC-1, a GTPase-activating protein for Rho, is associated with cell proliferation, morphology, and migration in human hepatocellular carcinoma. Biochem Biophys Res Commun 2007;355:72-77.

32. Seng TJ, Low JS, Li H, et al. The major 8p22 tumor suppressor DLC1 is frequently silenced by methylation in both endemic and sporadic nasopharyngeal, esophageal, and cervical carcinomas, and inhibits tumor cell colony formation. Oncogene 2007;26:934-944.

33. Schmitz KJ, Wohlschlaeger J, Lang H, et al. Activation of the ERK and AKT signalling pathway predicts poor prognosis in hepatocellular carcinoma and ERK activation in cancer tissue is associated with hepatitis C virus infection. J Hepatol 2008;48:83-90.

34. Altomare DA, Testa JR. Perturbations of the AKT signaling pathway in human cancer. Oncogene 2005;24:7455-7464.

35. Wong CC, Wong CM, Ko FC, et al. Deleted in liver cancer 1 (DLC1) negatively regulates Rho/ROCK/MLC pathway in hepatocellular carcinoma. PLoS ONE 2008;3:e2779.

36. Healy KD, Hodgson L, Kim TY, et al. DLC-1 suppresses non-small cell lung cancer growth and invasion by RhoGAP-dependent and independent mechanisms. Mol Carcinog 2007.

Figure 1

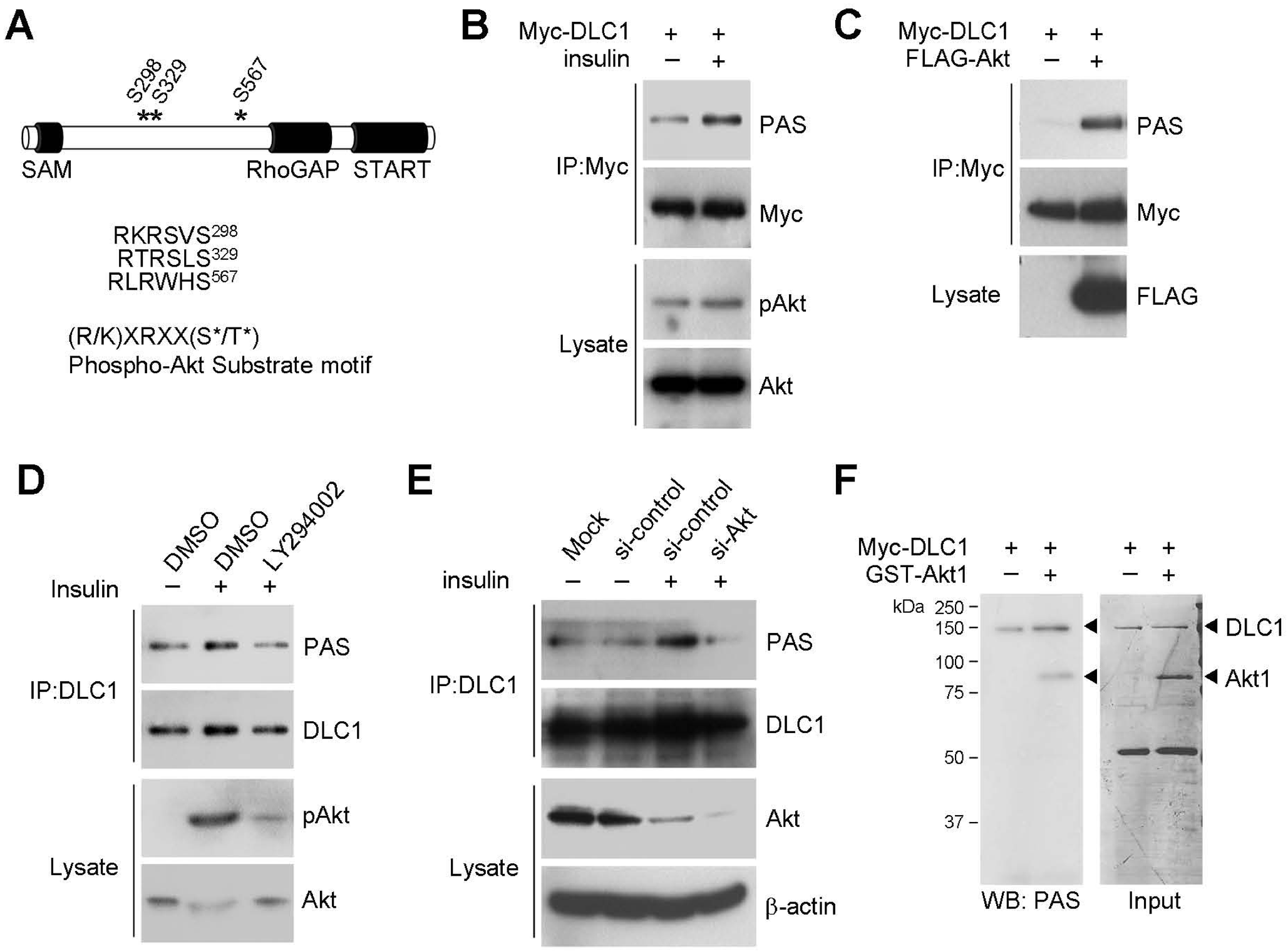
A
S298
S329
S567
**
*
SAM
RhoGAP
START
RKRSVS298
RTRSLS329
RLRWHS567
(R/K)XRXX(S*/T*)
Phospho-Akt Substrate motif
B
Myc-DLC1 + +
insulin – +
PAS
IP:Myc
Myc
pAkt
Lysate
Akt
C
Myc-DLC1 + +
FLAG-Akt – +
PAS
IP:Myc
Myc
Lysate
FLAG
D
DMSO
DMSO
LY294002
Insulin – + +
PAS
IP:DLC1
DLC1
pAkt
Lysate
Akt
E
Mock
si-control
si-control
si-Akt
insulin – – + +
PAS
IP:DLC1
DLC1
Akt
Lysate
β-actin
F
Myc-DLC1 + + + +
GST-Akt1 – + – +
kDa 250
150
100
75
50
37
DLC1
Akt1
WB: PAS
Input

Figure 2

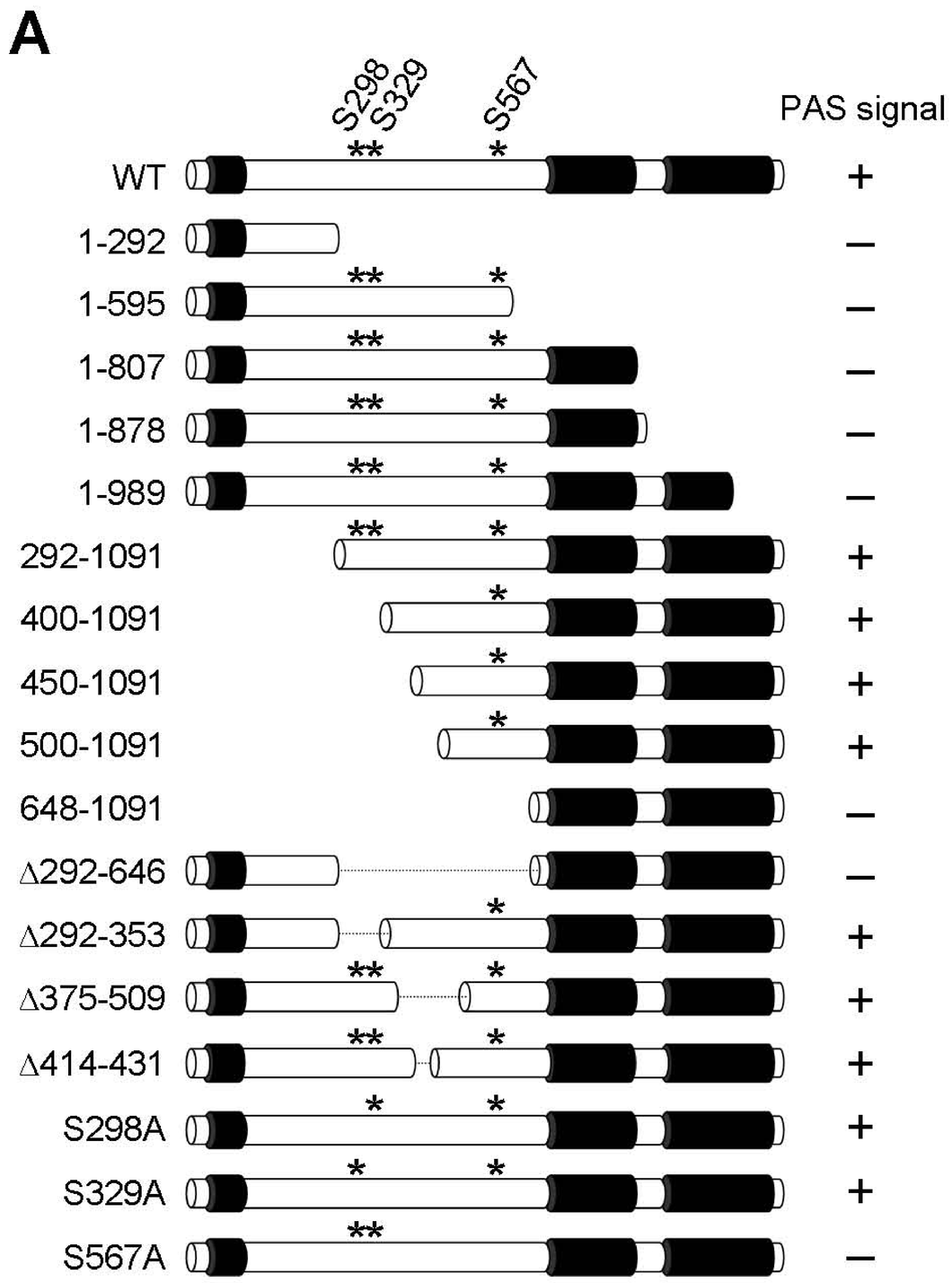
A
S298
S329
S567
PAS signal
WT
1-292
1-595
1-807
1-878
1-989
292-1091
400-1091
450-1091
500-1091
648-1091
Δ292-646
Δ292-353
Δ375-509
Δ414-431
S298A
S329A
S567A

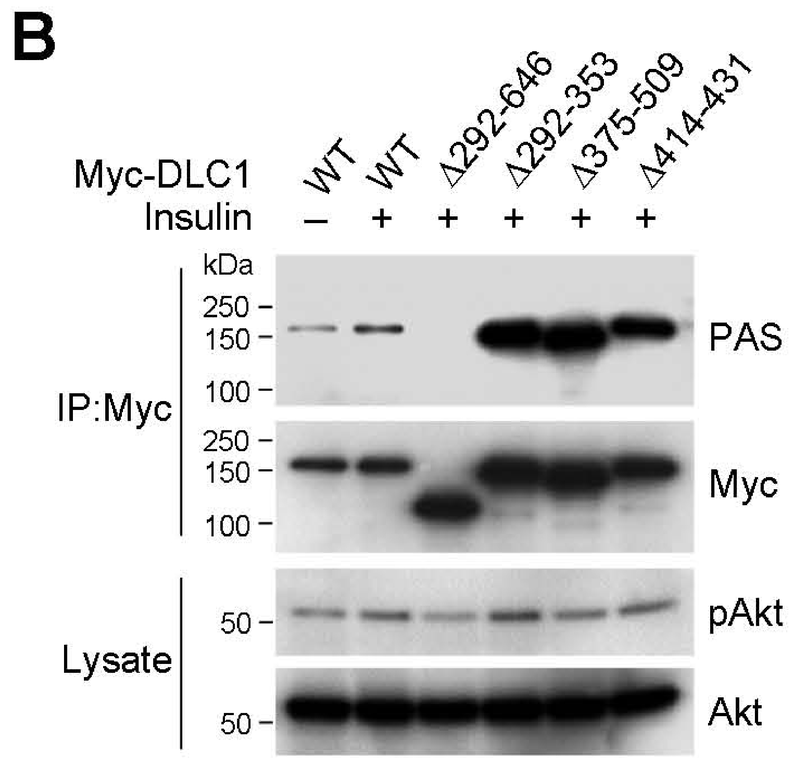
B
Myc-DLC1
Insulin
WT
WT
Δ292-646
Δ292-353
Δ375-509
Δ414-431
kDa
250
150
100
IP:Myc
PAS
Myc
Lysate
50
pAkt
Akt

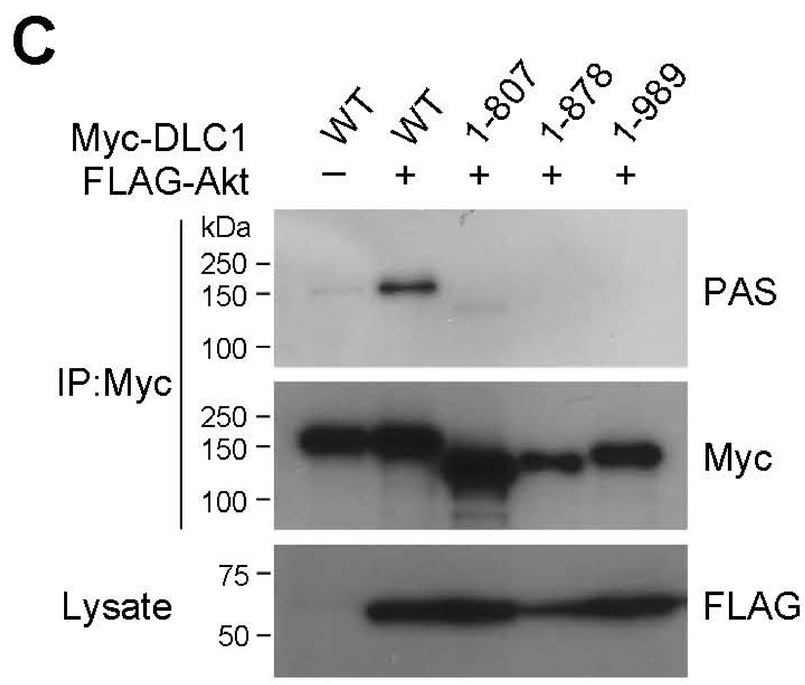
C
Myc-DLC1
FLAG-Akt
WT
WT
1-807
1-878
1-989
kDa
250
150
100
IP:Myc
PAS
Myc
Lysate
75
50
FLAG

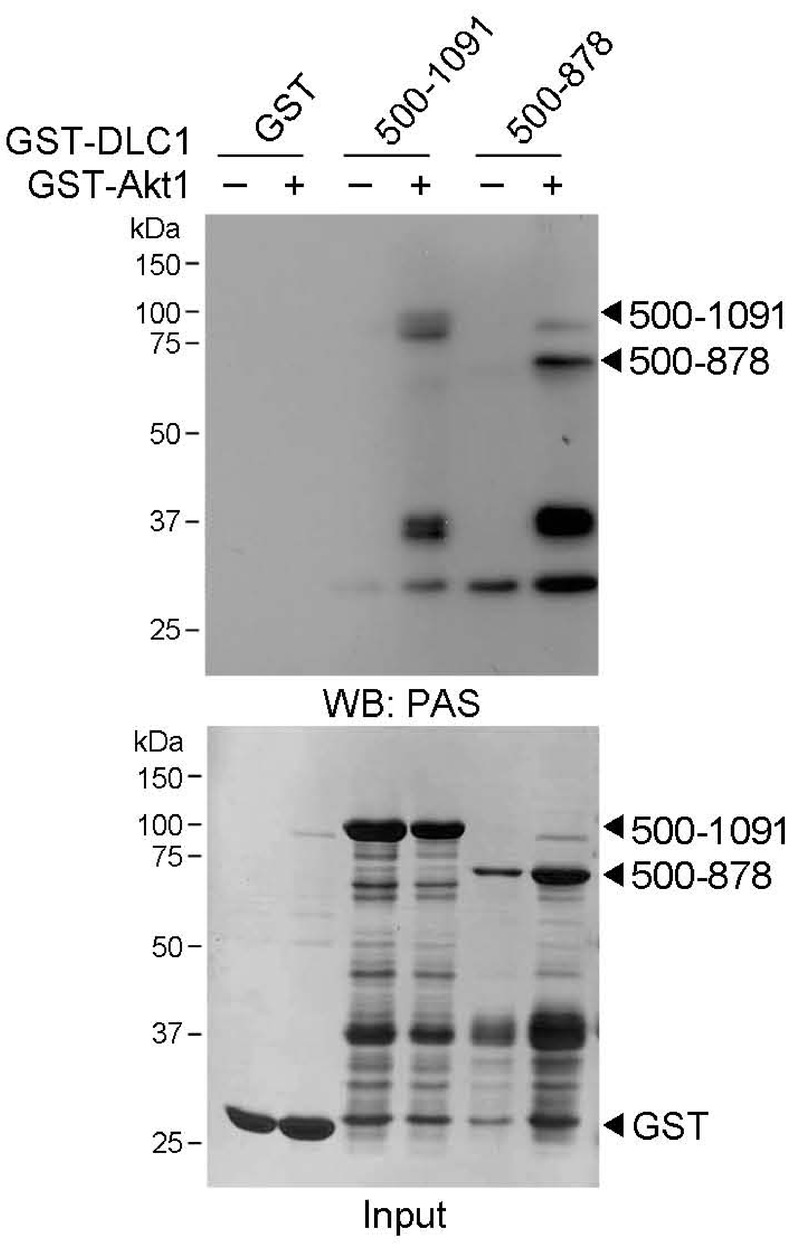
D
GST-DLC1
GST-Akt1
GST
500-1091
500-878
kDa
150
100
75
50
37
25
500-1091
500-878
WB: PAS
kDa
150
100
75
50
37
25
500-1091
500-878
GST
Input

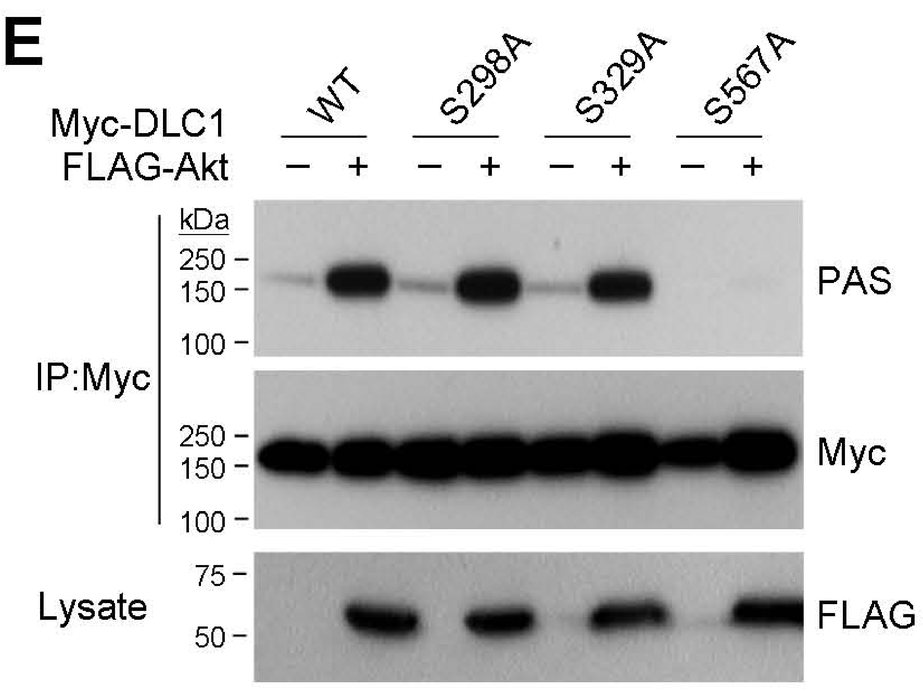
E
Myc-DLC1
FLAG-Akt
WT
S298A
S329A
S567A
kDa
250
150
100
IP:Myc
PAS
Myc
Lysate
75
50
FLAG

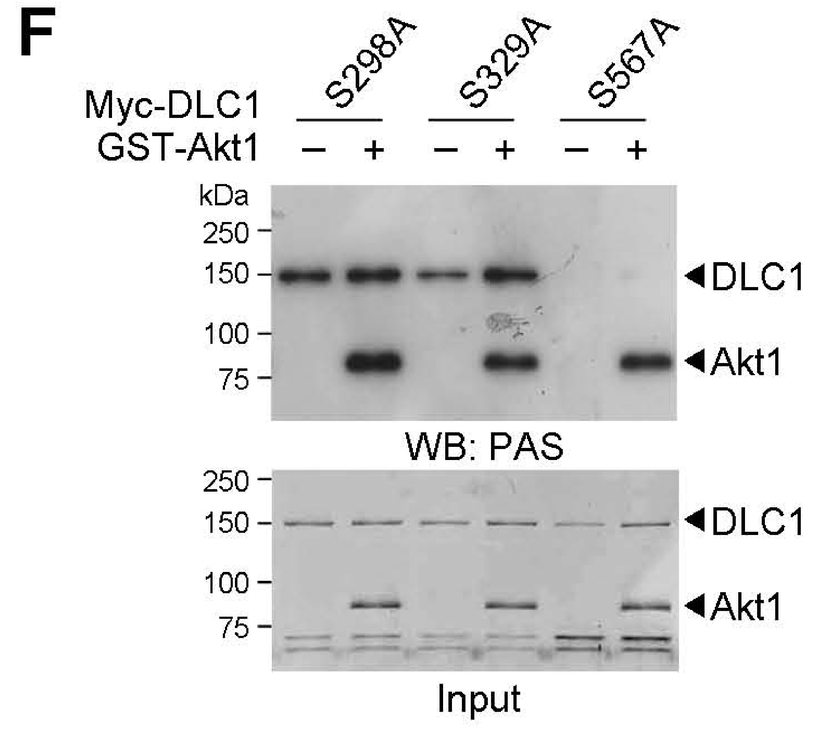
F
Myc-DLC1
GST-Akt1
S298A
S329A
S567A
kDa
250
150
100
75
DLC1
Akt1
WB: PAS
250
150
100
75
DLC1
Akt1
Input

Figure 3

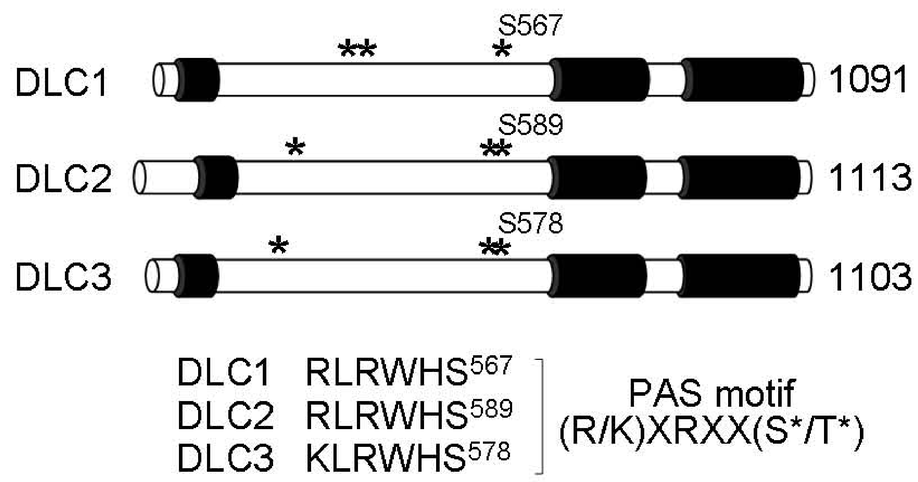
A
S567
DLC1
1091
S589
DLC2
1113
S578
DLC3
1103
DLC1 RLRWHS567
DLC2 RLRWHS589
DLC3 KLRWHS578
PAS motif
(R/K)XRXX(S*/T*)

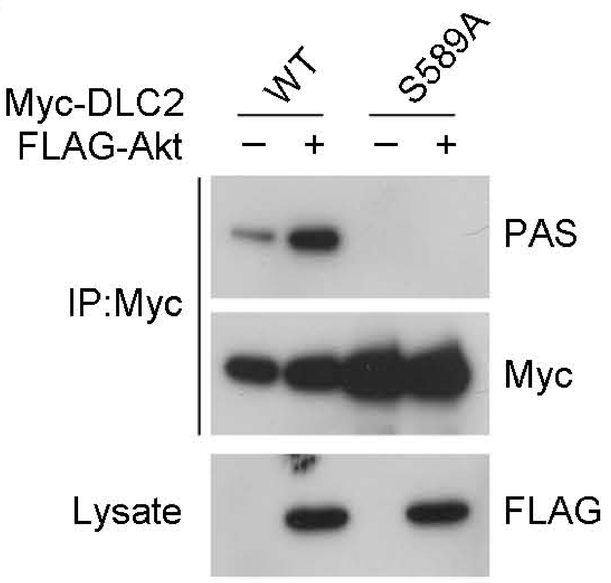
B
Myc-DLC2
WT
S589A
FLAG-Akt
− + − +
IP:Myc
PAS
Myc
Lysate
FLAG

Figure 4

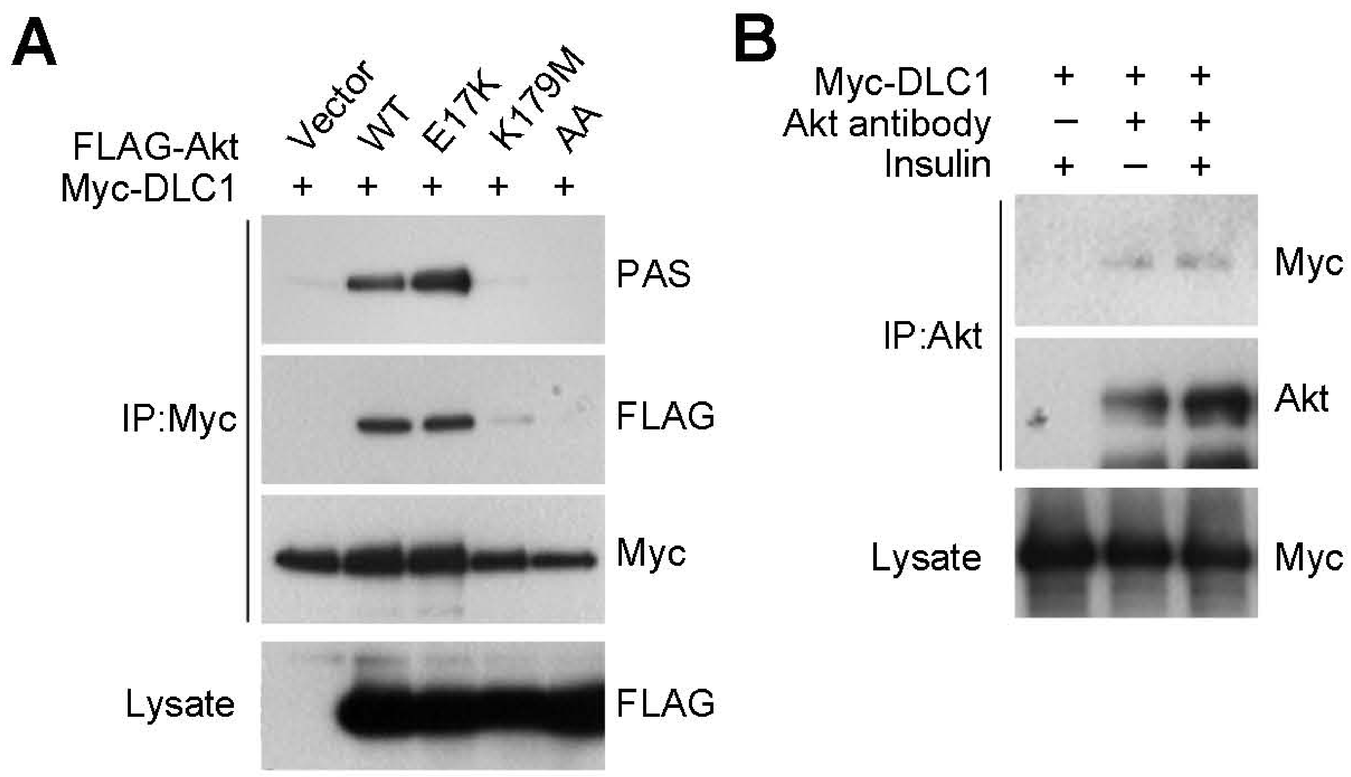
A
FLAG-Akt
Myc-DLC1
Vector
WT
E17K
K179M
AA
+ + + + +
IP:Myc
PAS
FLAG
Myc
Lysate
FLAG
B
Myc-DLC1 + + +
Akt antibody – + +
Insulin + – +
IP:Akt
Myc
Akt
Lysate
Myc

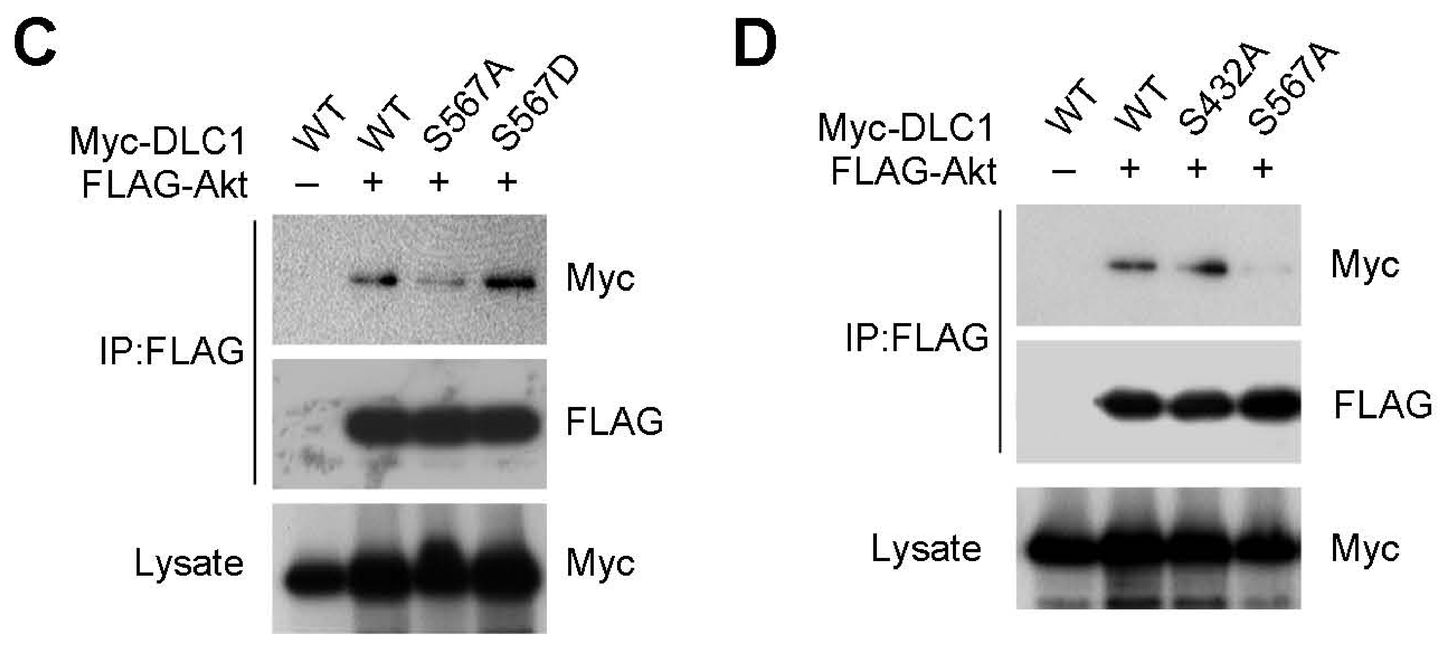
C
Myc-DLC1
FLAG-Akt
WT
WT
S567A
S567D
– + + +
IP:FLAG
Myc
FLAG
Lysate
Myc
D
Myc-DLC1
FLAG-Akt
WT
WT
S432A
S567A
– + + +
IP:FLAG
Myc
FLAG
Lysate
Myc

Figure 5

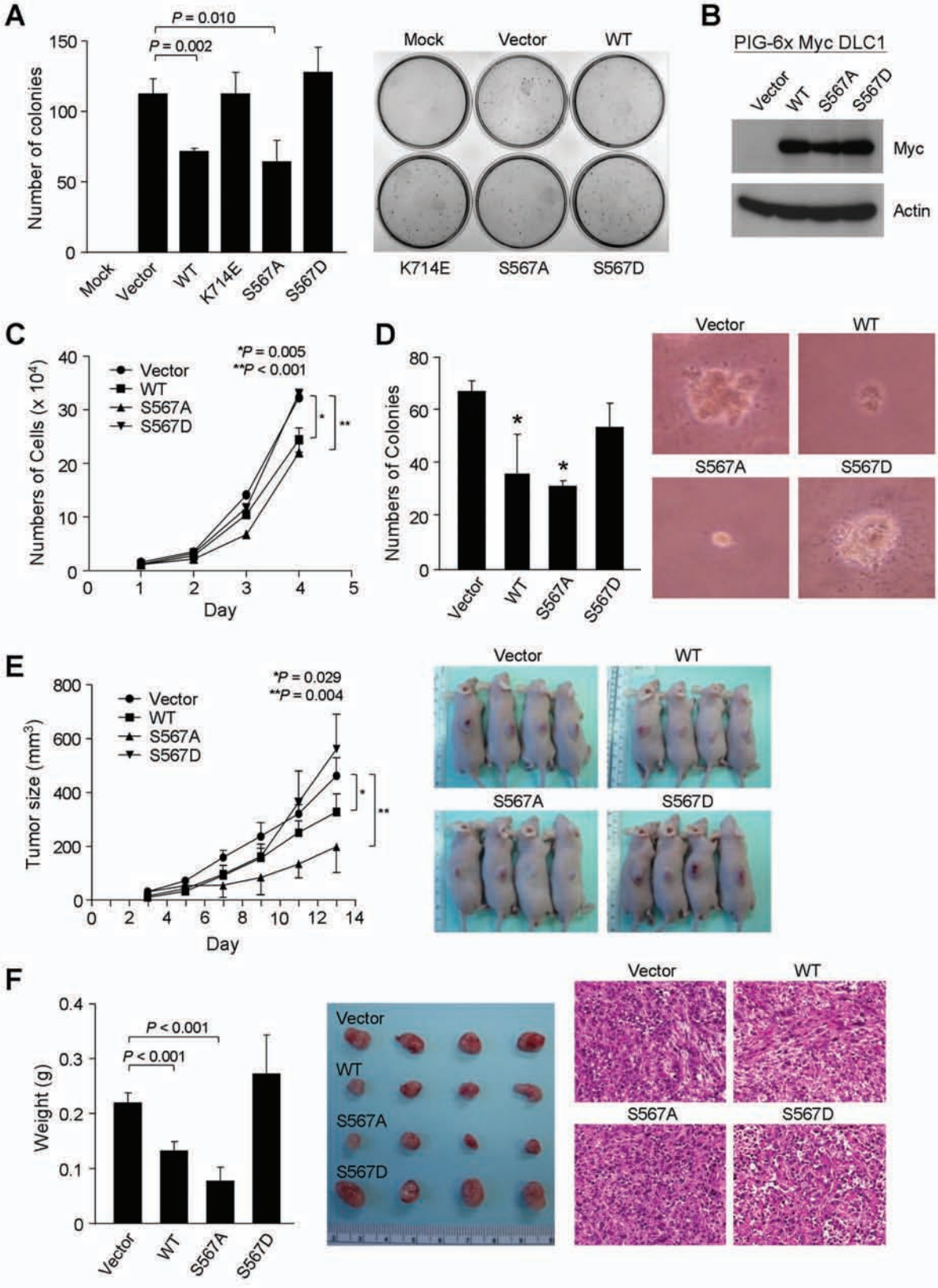
A
P = 0.010
P = 0.002
Number of colonies
150
100
50
0
Mock
Vector
WT
K714E
S567A
S567D
Mock
Vector
WT
K714E
S567A
S567D
B
PIG-6x Myc DLC1
Vector
WT
S567A
S567D
Myc
Actin
C
*P = 0.005
**P < 0.001
Vector
WT
S567A
S567D
Numbers of Cells (x 10^4)
40
30
20
10
0
0
1
2
3
4
5
Day
D
Numbers of Colonies
80
60
40
20
0
Vector
WT
S567A
S567D
Vector
WT
S567A
S567D
E
*P = 0.029
**P = 0.004
Vector
WT
S567A
S567D
Tumor size (mm^3)
800
600
400
200
0
0
2
4
6
8
10
12
14
Day
Vector
WT
S567A
S567D
F
P < 0.001
P < 0.001
Weight (g)
0.4
0.3
0.2
0.1
0
Vector
WT
S567A
S567D
Vector
WT
S567A
S567D
Vector
WT
S567A
S567D

Figure 6

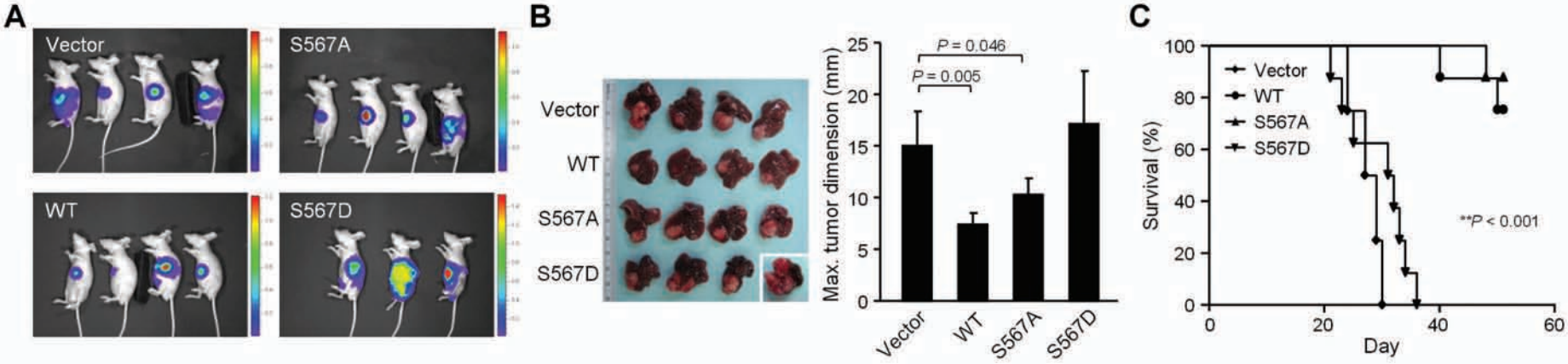

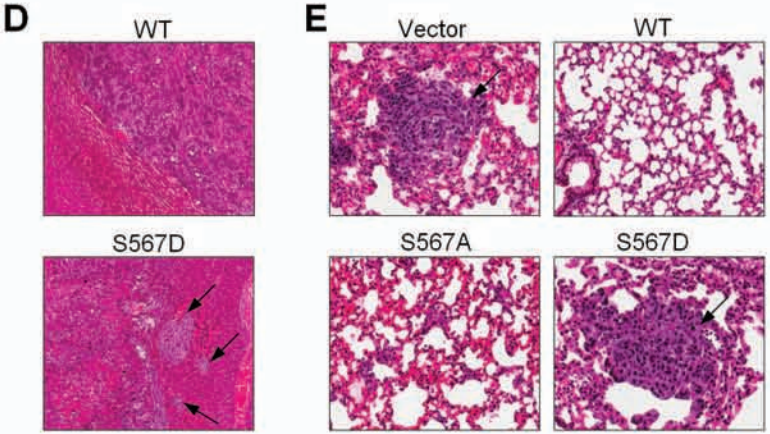

F

	Number of tumors with aggressive features				
	Venous invasion	Microsatellite formation#	Lung metastasis	Big foci formation	Total no. of big foci*
Vector	1/4	1/4	2/4	2/4	12
WT	0/4	1/4	0/4	0/4	0
S567A	1/4	0/4	2/4	1/4	2
S567D	1/4	3/4	4/4	3/4	10

Multiple foci were formed in S567D group while single focus was found in vector and WT groups

* Big focus represents a focus consisting of more than 10 tumor cells

Figure 7

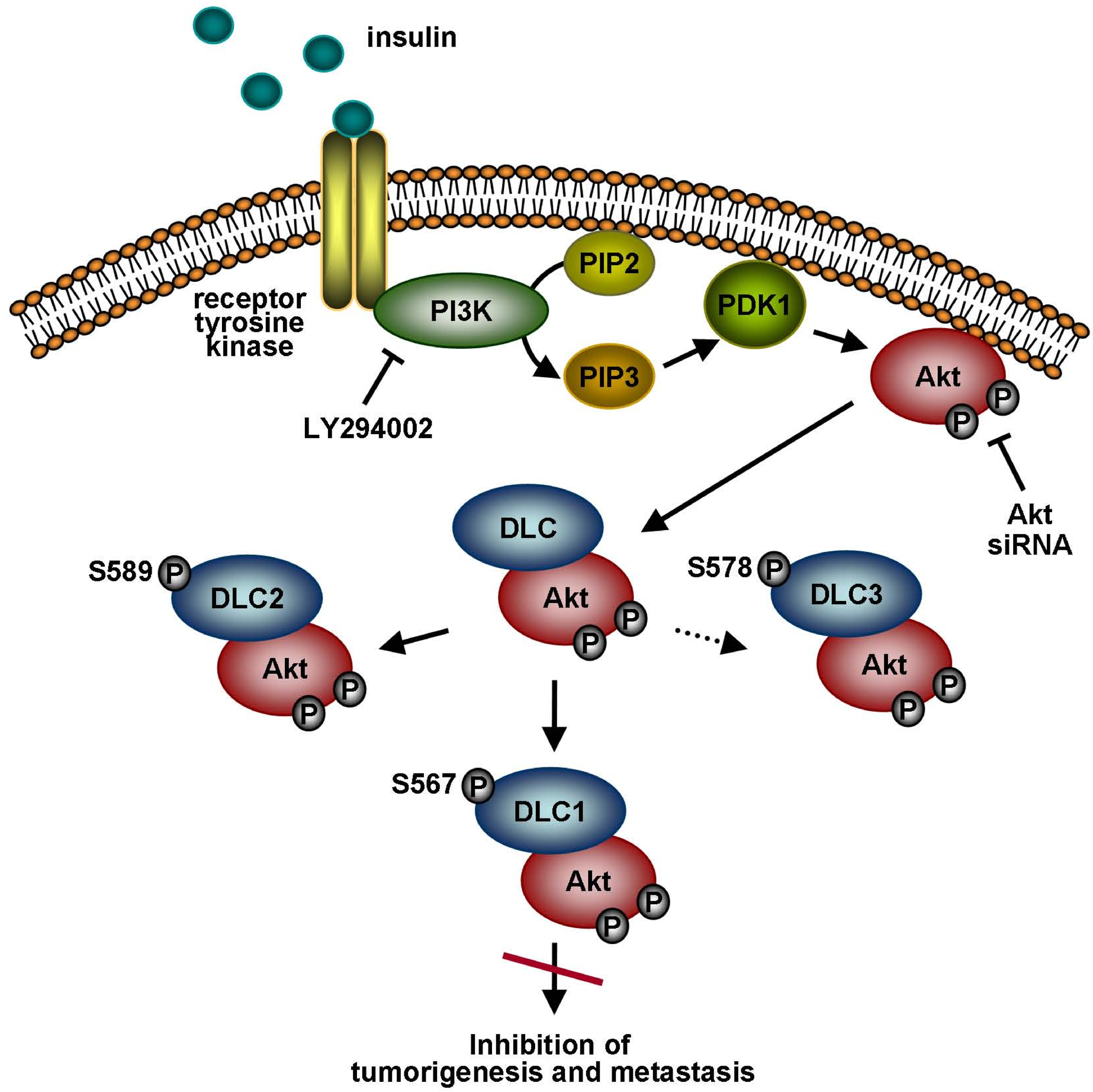
insulin
receptor tyrosine kinase
PI3K
PIP2
PIP3
PDK1
Akt
P
P
LY294002
Akt siRNA
DLC
Akt
P
P
S589 P
DLC2
Akt
P
P
S578 P
DLC3
Akt
P
P
S567 P
DLC1
Akt
P
P
Inhibition of
tumorigenesis and metastasis

Supplementary Materials and Methods

Colony formation assay

PLC cells of 1×10^5 were seeded per well of 12-well tissue culture plates. DLC1 expression vector (pCS2+MT, DLC1-pCS2+MT, DLC1S567A-pCS2+MT or DLC1S567D-pCS2+MT) was co-transfected with FLAG-Akt into cells. Cells were trypsinized and replated in a 1:20 dilution in triplicates one day after transfection. Cells were selected in 900 μg/ml of G418 (Merck, Darmstadt, Germany) for 3 weeks. Colonies formed were fixed with 3.7% formaldehyde and stained with crystal violet solution.

Establishment of stable mouse p53-/-; Akt hepatoblast expressing DLC1 and its mutants

MSCV-PGK-PIG retroviral constructs of wild-type and mutant DLC1 were transfected into PA317 cells for retroviral packaging. Viral particles were collected from the medium. Mouse *p53-/-; Akt* hepatoblast cell were transduced by retroviral particles in presence of polybrene[1]. Stable cell lines were established under 1ug/ml puromycin selection for 1-2 weeks.

Proliferation curve

Cells were seeded at 1×10^4 cells per well of 12-well culture plates in triplicates and maintained in growth medium. Cell numbers were counted by using a hematocytometer at 24-hr intervals for 5 days. Mean values and standard deviations of the triplicates were calculated and plotted against time.

Flow cytometry

Mouse p53-/-; RasV12 and p53-/-; Akt hepatoma cells stably expressing DLC1 and its mutants were fixed with 0.5% paraformaldehyde in PBS and permeabilized with 70% ethanol.

Cells were then stained with propidium iodide and DNA profile of cell populations was determined by flow cytometry and analyzed by WINMDI version 2.9. Apoptotic cells were defined as cells in subG1 population. Percentage of cells in subG1 phase in each stable clone was determined. Data represent the mean of triplicates and standard deviation was calculated.

Terminal decxynucleotidyl transferase-mediated dUTP nick-end labeling (TUNEL) assay

Cells with at 1×10^4 were seeded on coverslip in 12-well culture plate and cultured for 2 days. The cells on coverslip were fixed with 4% paraformaldehyde. TUNEL assay (*in situ* cell death detection kit, TMR red) was then performed according to the manufacturer's manual (Roche).

Immunofluorescence staining

To reveal the subcellular localization of Myc- and FLAG-DLC1 in SMMC-7721 cells, transfected cells were fixed with paraformaldehyde and permeabilized with Triton-X-100. DLC1 was stained with either Myc (Santa Cruz Biotechnology) or FLAG (Sigma-Aldrich) antibodies. The endogenous vinculin was stained by vinculin antibody (Sigma). Stress fibers formation was induced by serum induction for an hour and the F-actin was visualized by tetramethylrhodamine B isothiocyanate (TRITC)-labeled phalloidin (Sigma). Subsequent to primary antibody incubation, cells were washed and stained with flourochrome-conjugated secondary antibodies. Images were captured by a Leica Q550CW fluorescence microscope (Leica, Wetzler, Germany). Experimental details have been described elsewhere16.

Rhotekin pull down assay

The RhoA activity levels in DLC1 transiently transfected cells and in DLC1 stable hepatoma cells were detected using a Rho Activation Assay Biochem Kit (Cytoskeleton) as described elsewhere16. Cells were serum-starved for 24 hours and stimulated with lysophosphatidic

acid. Cell lysate was then collected and subjected to GST-RBD pull-down. The pull-down samples were subjected to SDS-PAGE analysis and the level of active RhoA was revealed by RhoA antibody.

References

1. Zender L, Spector MS, Xue W, et al. Identification and validation of oncogenes in liver cancer using an integrative oncogenomic approach. Cell 2006;125:1253-1267.

Supplementary Table 1 Primers used for cloning expression plasmids.

Primer	Sequence (5'-3')
DLC1-NcoI354-F	GTCCCCATGGTGGAGCAGAACTTTAAGAAC
DLC1-NcoI647-F	GTCCCCATGGTGCAGCGCACAGGACAACCG
DLC1-EcoRI-400F	TAGAATTCGAACTGGAGGACGGGAAGC
DLC1-EcoRI-450F	TAGAATTCGCTCTACTCCAGTTCAGGG
DLC1-EcoRI-500F	TAGAATTCGCTGGACTCGGTCTCTCCC
DLC1-878-SalIR	TAGTCGACATTACCCAGGTGCCCGA
DLC1-374-R	TTCAGGGATGTAGAACACCG
DLC1-510-F	CCAAAACAGATACACCTGG
DLC1-873-R	GAGTGCTTCCAGAGTGAGG
DLC1-S298A-F	GAGGAGCGTTGCCAACTCCACGCAGACC
DLC1-S298A-R	GGTCTGCGT GGAGTTGGCAACGCTCCTC
DLC1-S329A-F	CCCGGAGCCTCGCTGCGTGCAACAAGC
DLC1-S329A-R	GCTTGTTGCACGCAGCGAGGCTCCGGG
DLC1-S432A-F	CTGAAGAGACGCAATTCTGCCAGCTCCATGAGC
DLC1-S432A-R	GCTCATGGAGCTGGCAGAATTGCGTCTCTTCAG
DLC1-S567A-F	CTGAGATGGCACGCTTTCCAGAGCTCAC
DLC1-S567A-R	GTGAGCTCTGGAAAGCGTGCCATCTCAG
DLC1-S567D-F	CTGAGATGGCACGATTTCCAGAGCTCAC
DLC1-S567D-R	GTGAGCTCTGGAAATCGTGCCATCTCAG
DLC2-S589A-F	GACTCCGATGGAACGCTTTCCAGCTGTCG
DLC2-S589A-R	CGACAGCTGGAAAGCGTTCCATCGGAGTC
DLC2-313ERI-F	CAGAATTCGCCGCCACCTG
DLC2-stopSalI-R	TGGTCGACTCAGATTTTAGTTTCTGG
BHI-Akt1-F	GTGGATCCATGAGCGACGTGGCTATTGTGAAGG
ERI-Akt1-R	GGAATTCTCAGGCCGTGCCGCTGGCCGAG
Akt1-E17K-F	CAAACGAGGGAAGTACATCAAGACC
Akt1-E17K-R	GGTCTTGATGTACTTCCCTCGTTTG
Akt1-K179M-F	CTACTACGCCATGATGATCCTCAAG
Akt1-K179M-R	CTTGAGGATCATCATGGCGTAGTAG
Akt1-T308A-F	GCCACCATGAAGGCCTTTTGCGGCAC
Akt1-T308A-R	GTGCCGCAAAAGGCCTTCATGGTGGC
Akt1-S473A-F	CTTCCCCCAGTTCGCCTACTCGGCCAGCG
Akt1-S473A-R	CGCTGGCCGAGTAGG CGAACTGGGGGAAG

Supplementary Figure Legends

Supplementary Figure 1. Phosphorylation signal of DLC1 was detected by PAS antibody. Lysates of HEK293 cells transiently transfected with Myc-DLC1 and with insulin stimulation were treated with shrimp alkaline phosphatase (SAP). Cell lysates were then immunoprecipitated with Myc antibody and immunoblotted with PAS antibody. Positive band detected by PAS antibody decreased dramatically upon SAP treatment indicates that the positive band detected by PAS is phosphorylation signal.

Supplementary Figure 2. Positive control of the *in vitro* kinase assay. Recombinant GSK was incubated with ATP with or without GST-Akt. The reaction mix was then subjected to western blotting using PAS and phospho-GSK3β antibodies. GSK was highly phosphorylated with the presence of GST-Akt. PAS antibody detected positive signal in both Akt and GSK while phospho-GSK3β antibody only detect phosphorylation signal in GSK.

Supplementary Figure 3. Mapping of Akt phosphorylation residue(s) of DLC1. (*A*) Detection of PAS signal in the N-terminal deletion mutants, 400-1091, 450-1091 and 500-1091 suggests that phosphorylation residue(s) resides in the C-terminal of DLC1. (*B*) Positive signal was only detected in 292-1091 mutant. Loss of PAS signal in 1-595 in which S567 was retained suggested that the presence of C-terminal half of DLC1 was essential for Akt phosphorylation o f DLC1.

Supplementary Figure 4. Growth suppression activity of DLC1 was suppressed in cells with high Akt background. (*A*) Colony formation assay. DLC1 constructs were co-expressed with

Akt in PLC cells and grown in selective medium for 2 weeks. Numbers of colonies formed were counted. (*B*) Stable expression of DLC1 in p53-/-; Akt hepatoma cells. DLC1 expression in stable clones was detected by Western blot analysis using Myc antibody. (*C*) Growth curves. wildtype DLC1 lost its growth inhibitory activity while the phospho-defective mutant S567A retained its growth inhibitory activity.

Supplementary Figure 5. Akt phosphorylation inhibited the activity of DLC1 to induce apoptosis. DNA profile of mouse (*A*) $p53^{-/-}$;RasV12 and (*C*) $p53^{-/-}$;Akt hepatoma cells stably expressing DLC1 and its mutants were determined by flow cytometry. Percentage of cells in subG1 phase was determined. Wild-type DLC1 and S567A mutant significantly induced subG1 population when compared with vector control and S567D mutant in $p53^{-/-}$;RasV12 cells. The apoptosis-inducing ability of wild-type DLC1 was reduced in $p53^{-/-}$;Akt cells. (*B and D*) Apoptosis was measured by TUNEL staining. The number of TUNEL-stanined cells was significantly higher in $p53^{-/-}$;RasV12 cells expressing wild-type DLC1 and S567A. In $p53^{-/-}$;Akt cells, the number of TUNEL-stained cells in wild-type DLC1 expressing cells was similar to that of the vector control and S567D mutant. Data was analyzed by student's *t*-test and $P<0.05$ was considered as statistically significant.

Supplementary Figure 6. Focal adhesion localization and RhoGAP activity of DLC1 were not affected by S567 phosphorylation. (*A*) Focal adhesion localization of DLC1 and its mutants. SMMC-7721 cells were seeded on coverslips and transfected with different FLAG-DLC1 constructs (WT, S567A and S567D). The cells were fixed and co-stained with FLAG antibody (green), vinculin antibody (red) and DAPI (blue). Vinculin is used as a marker for focal adhesions while DAPI stained with nucleus. All wild-type DLC1, S567A and S567D co-localized with vinculin at focal adhesions. (*B*) Stress fiber inhibition assays of wild-type

DLC1, S567A and S567D mutants. SMMC-7721 cells transfected with Myc-DLC1 constructs were induced by serum for an hour. The cells were fixed and immunofluorescence staining was performed. Cells were co-stained with Myc antibody (green), TRITC-phalloidin (red) and DAPI (blue) followed by fluorochrome-conjugated secondary antibodies. The asterisks denote the DLC1-transfected cells. Scale bar = 10 μm. (*C*) Active RhoA level in stable DLC1 mouse hepatoma cells. Cells were serum-starved for 24 hours and stimulated with lysophosphatidic acid. Cell lysate was then collected and subjected to GST-RBD pull-down. The pull-down samples were subjected to SDS-PAGE analysis and the level of active RhoA was revealed by RhoA antibody.

Supplementary Figure 1

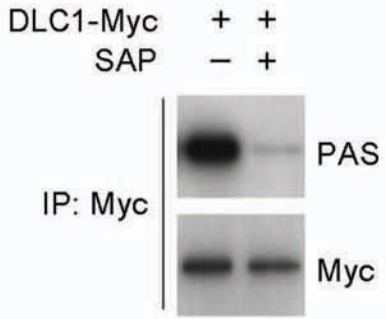

Supplementary Figure 2

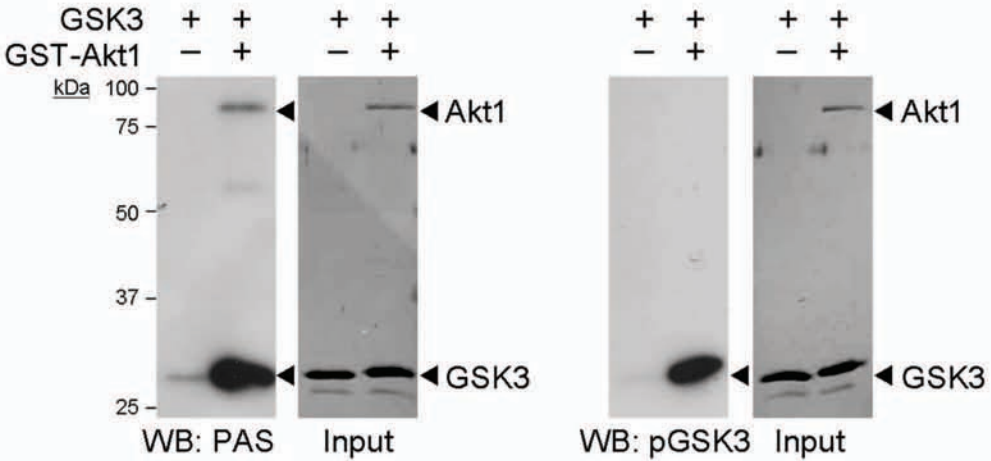

Supplementary Figure 3

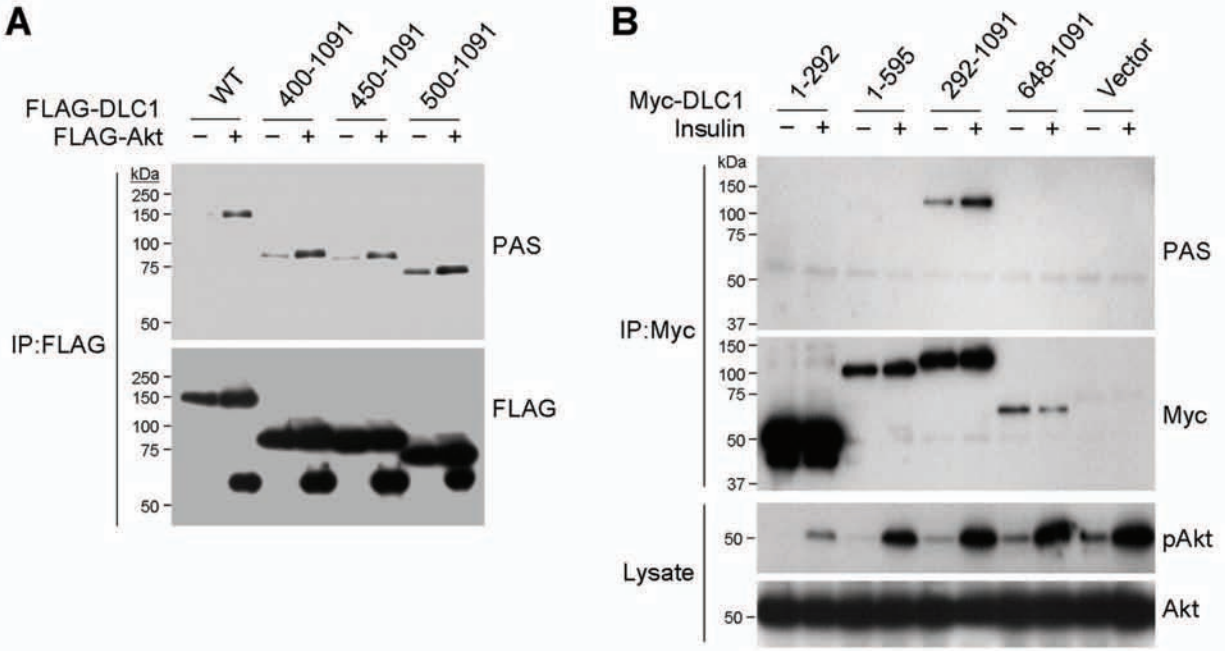

Supplementary Figure 4

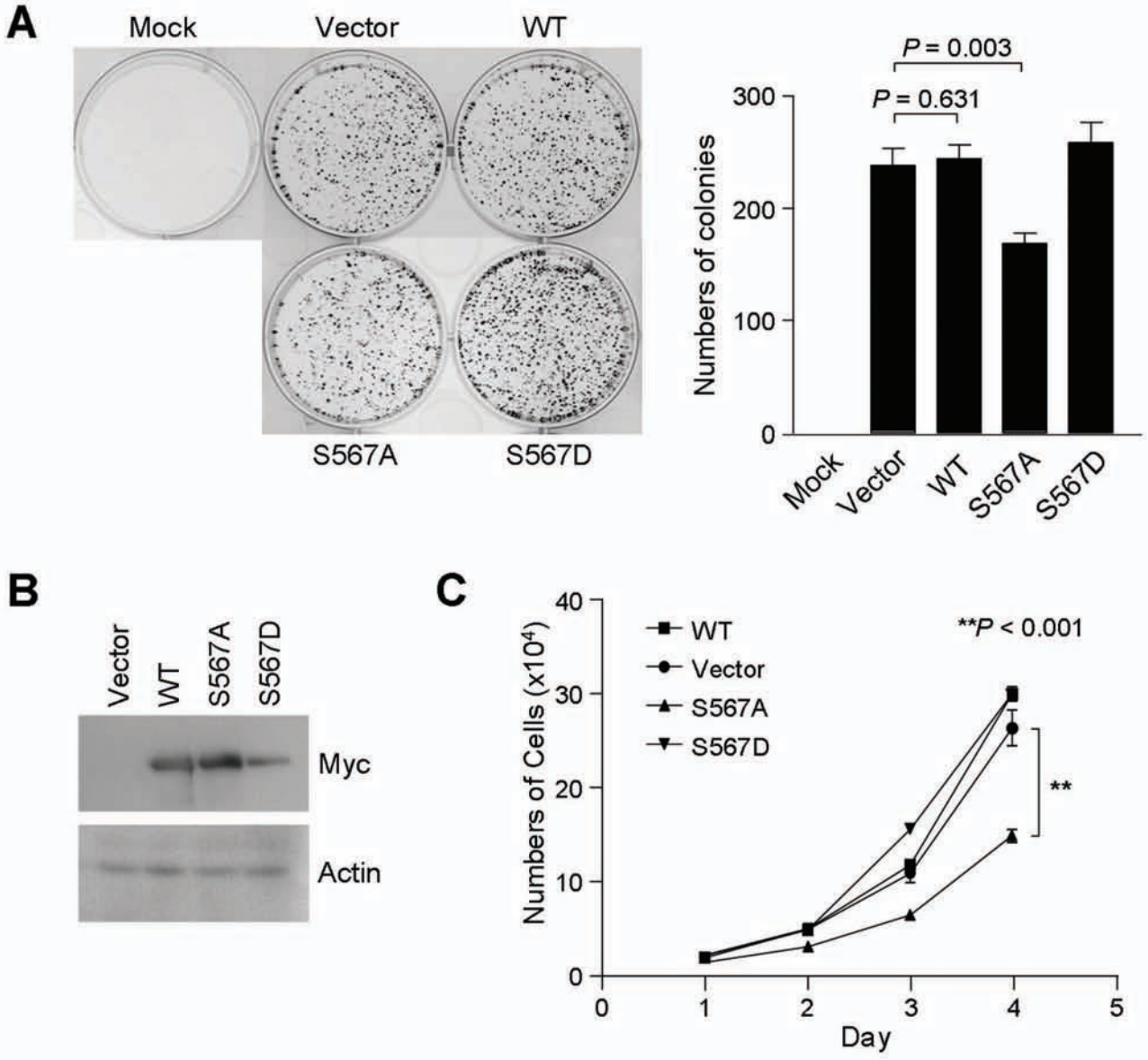

Supplementary Figure 5

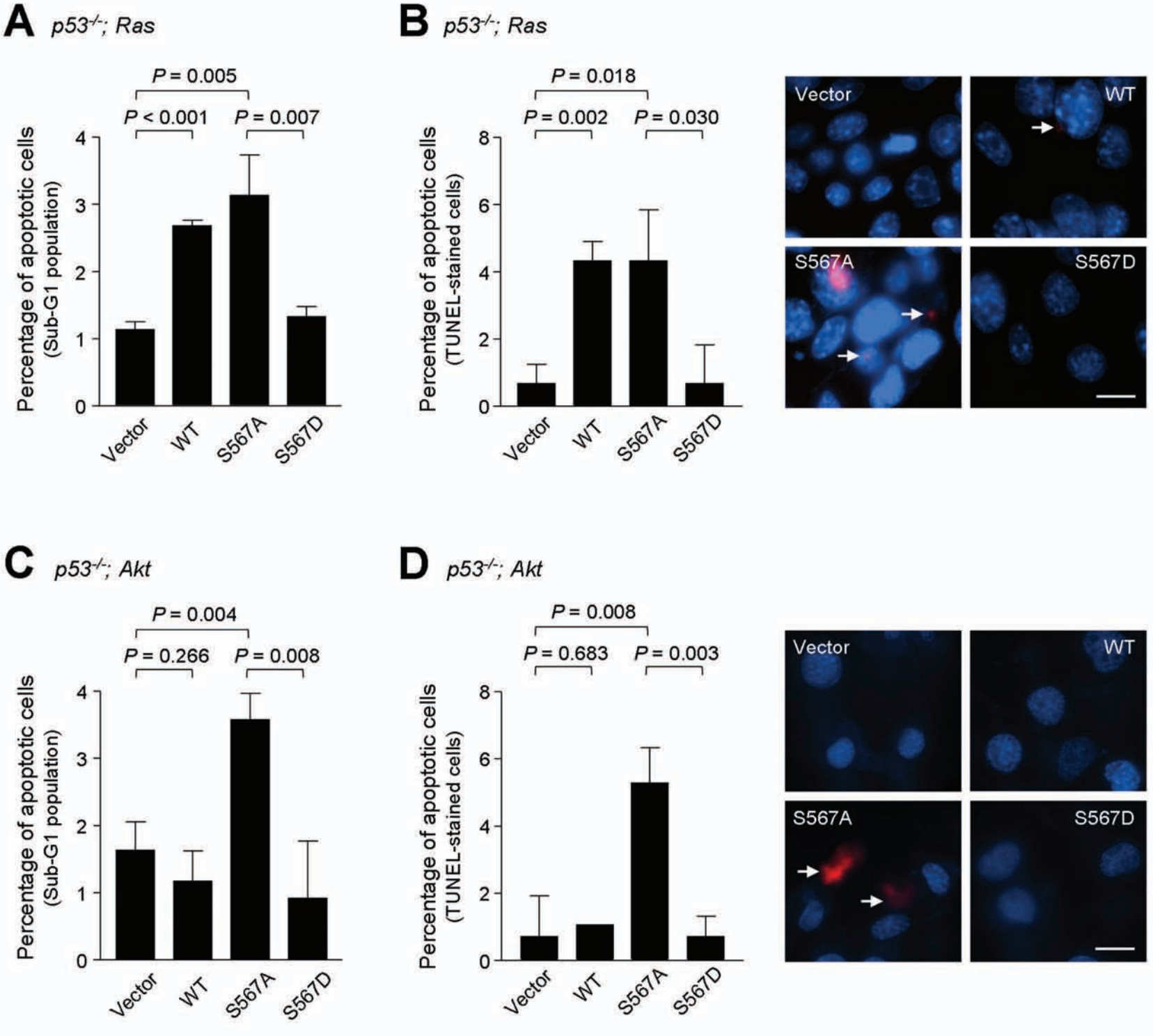

Supplementary Figure 6